Electronic Supplementary Material (ESI) for New Journal of Chemistry.
This journal is © The Royal Society of Chemistry and the Centre National de la Recherche Scientifique 2019

Supporting Information

Branched Versus Linear: Side-Chain Effect on Fluorinated Wide Bandgap Donors and Their Applications in Organic Solar Cells

Tainan Duan, Ru-Ze Liang,* Yingying Fu, Yuying Chang, Zhipeng Kan, Cheng Zhong, Zhiyuan Xie, Donghong Yu**

**To whom correspondence should be addressed. Email: tnduan@cigit.ac.cn, ruze.liang@kaust.edu.sa and yu@bio.aau.dk.*

Content:

1. General Experimental Details 2

2. Synthetic Protocols and Characterizations 3

3. Density Functional Theory (DFT) Calculations 8

4. Photoelectron Spectroscopy in Air (PESA) Measurements 9

5. Internal Quantum Efficiency (IQE) 10

6. Carrier Mobility Measurements 11

7. Solution NMR Spectra 12

8. Supporting Information References 33

1. General Experimental Details

All reactions were performed under nitrogen atmosphere. Solvents were purified and dried from appropriate drying agents using standard techniques prior to use. Reagents available from commercial sources were used without further purification unless otherwise stated. Flash chromatography was performed by using Silicycle Silica Flash P60 (particle size 40-63 μm, 60 Å, 230-400 mesh) silica gel. Silica gel on TLC-PET foils from VWR was used for TLC. All compounds were characterized by NMR spectroscopy on Bruker Avance III Ultrashield Plus instruments (400 MHz or 600 MHz). The spectra were referenced on the internal standard TMS. High-resolution mass spectrometry (HRMS) data was recorded using a Thermo Scientific-LTQ Velos Orbitrap MS. Note: Spectroscopy-grade $CHCl_3$ was filtered through basic alumina prior to use in order to suppress solvent acidity and avoid undesired protonation reactions that may influence the spectral absorption of the molecular acceptors described in this study.

2. Synthetic Protocols and Characterizations

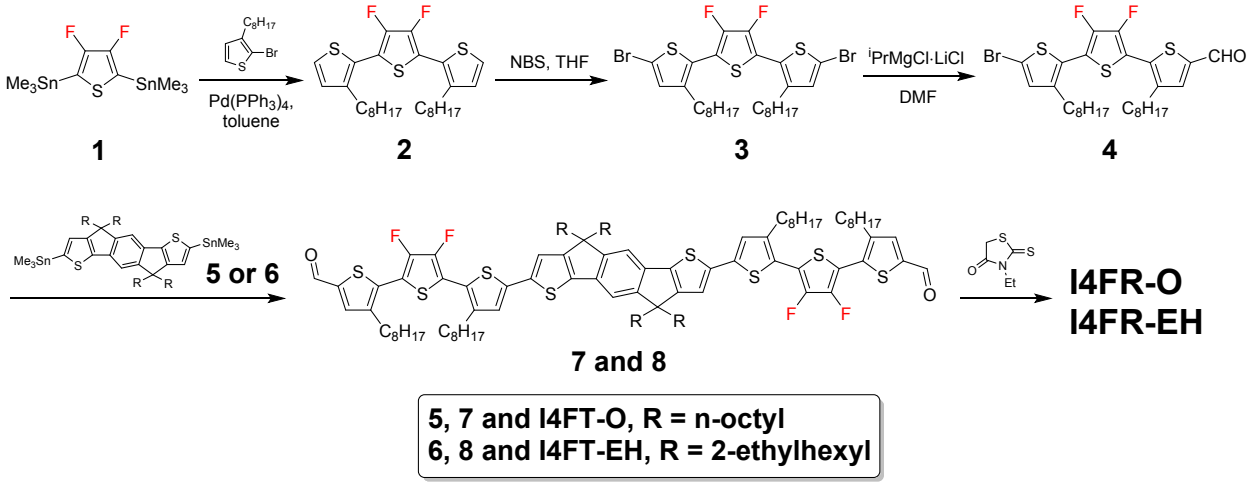

Scheme S1. Synthesis of the SM donors.

Note: Compounds **1**[1], **5**[2] and **6**[3] were prepared according to previously report procedures.

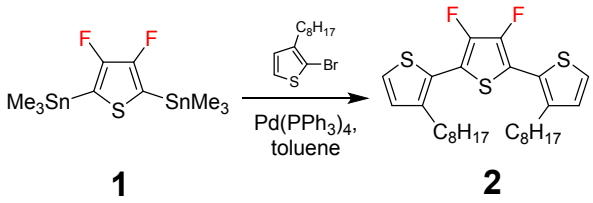

3',4'-difluoro-3,3''-dioctyl-2,2':5',2''-terthiophene (2): In a pre-dried Schlenk tube, **1** (2.680 g, 6.00 mmol), 2-bromo-3-octylthiophene (3.990 g, 14.4 mmol), and $Pd(PPh_3)_4$ (0.692 g, 0.30 mmol) were dissolved with degassed toluene (60 mL). The mixture was heated at 110 °C for 24 h. The reaction mixture was allowed to cool down to room temperature, the organic layer was washed with brine, extracted with hexane, dried over Na_2SO_4, and then concentrated under reduced pressure. The crude product was purified by column chromatography over SiO_2 using hexane as eluent. The solvent was removed by rotary evaporation, affording compound **2** as a yellow oil (2.230 g, yield: 73%). ^{1}H NMR (400 MHz, $CHCl_3$, δ ppm): 7.37 (d, J = 5.2 Hz, 2H), 7.01 (d, J = 5.2 Hz, 2H), 2.73 (t, J = 7.6 Hz, 4H), 1.64-1.57 (m, 4H), 1.36-1.28 (m, 20H), 0.91-0.88 (m, 6H). ^{13}C NMR (100 MHz, $CHCl_3$, δ ppm): (142.83, 142.62, 140.20, 140.00), 142.55, 129.50, 126.32, 124.07, (113.17, 112.12, 113.07, 113.02), 31.99, 30.67, 29.61, 29.51, 29.37,

22.78, 14.18. ^{19}F NMR (376 MHz, $CDCl_3$, δ ppm): -133.71.HRMS: calcd. for $C_{28}H_{38}F_2S_3$ $[M+H]^+$: 509.21765, found 509.21733.

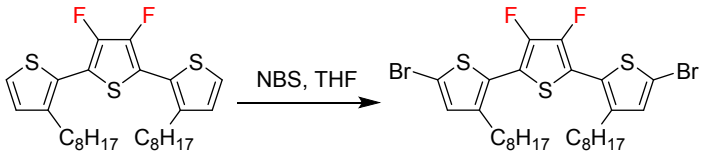

2 **3**

5,5''-dibromo-3',4'-difluoro-3,3''-dioctyl-2,2':5',2''-terthiophene (3): In a round-bottom flask, a solution of **2** (2.000 g, 3.93 mmol) in anhydrous THF (50 mL) was cooled with ice bath. To the solution, NBS (1.430 g, 8.06 mmol) was added slowly, and the mixture was stirred for overnight at room temperature. The reaction was quenched with water (60 mL) and the aqueous phase was extracted with dichloromethane (2 × 50 mL). The organic phase was collected, dried over Na_2SO_4, concentrated under reduced pressure, affording **3** as a pale yellow oil (2.460 g, yield: 94%) in high purity with no need for further purification. ^{1}H NMR (400 MHz, $CDCl_3$, δ ppm): 6.96 (s, 2H), 2.66 (t, J = 7.6 Hz, 4H), 1.64-1.57 (m, 4H), 1.36-1.28 (m, 20H), 0.91-0.87 (m, 6H). ^{13}C NMR (100 MHz, $CDCl_3$, δ ppm): 143.24, (142.94, 142.74, 140.30, 140.10), 132.19, 125.21, 113.54, (112.42, 112.36, 112.32, 112.27), 31.95, 30.45, 29.49, 29.43, 29.41, 29.30, 22.75, 14.16. ^{19}F NMR (376 MHz, $CDCl_3$, δ ppm): -132.77. HRMS (+APCI, m/z): calcd. for $C_{28}H_{36}Br_2F_2S_3$ $[M+H]^+$: 665.03867, found 665.03905.

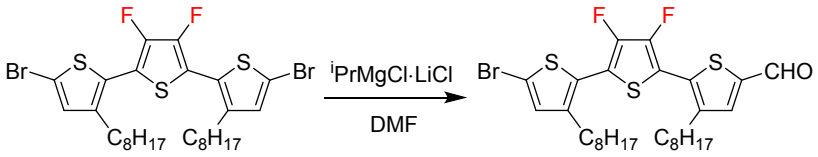

3 **4**

5''-bromo-3',4'-difluoro-3,3''-dioctyl-[2,2':5',2''-terthiophene]-5-carbaldehyde (4): In a pre-dried Schlenk tube, a solution of **3** (2.000 g, 3.0 mmol) in anhydrous THF (50 mL) was cooled to -0 °C. A solution of turbo Grignard reagent ^{i}PrMgCl.LiCl (1.3 M in THF, 2.5 mL, 3.2 mmol) was added dropwise, and the ice bath was removed. The mixture was stirred for 30 min at room temperature, and was then heated to reflux for 30 min. The heating bath was removed and anhydrous DMF (0.46 mL, 6.0 mmol) was added to the reaction mixture in one portion. After

being stirred overnight, the reaction was quenched with HCl (1 M in water, 20 mL) and the aqueous phase was extracted with chloroform (2 × 50 mL). The organic phase was, dried over Na_2SO_4 and then concentrated under reduced pressure. The crude product was purified by column chromatography over SiO_2 using hexanes/ethyl acetate (8:1) as the eluent. The solvent was removed by rotary evaporation, affording compound **4** as a brownish oil (1.310 g, yield: 71%). ^{1}H NMR (400 MHz, $CDCl_3$, δ ppm): 9.90 (s, 2H), 7.66 (s, 2H), 6.98 (s, 2H), 2.77 (t, J = 7.8 Hz, 2H), 2.68z (t, J = 7.8 Hz, 2H), 1.70-1.61 (m, 4H), 1.39-1.29 (m, 20H), 0.91-0.88 (m, 6H). ^{13}C NMR (100 MHz, $CDCl_3$, δ ppm): 182.57, 143.63, 143.15, (143.10, 142.96, 141.32, 141.19), 142.88, (142.58, 142.45, 140.82, 140.69), 137.83, 134.01, 132.32, 124.81, 113.94, (113.84, 113.76, 112.31, 112.23), 31.87, 30.39, 30.27, 29.46, 29.42, 29.36, 29.23, 22.68, 14.11. ^{19}F NMR (564 MHz, $CDCl_3$, δ ppm): (-129.57, -129.60), (-132.44, -132.46). HRMS (+APCI, m/z): calcd. for $C_{28}H_{37}BrF_2OS_3$ $[M+H]^+$: 615.12307, found 615.12329.

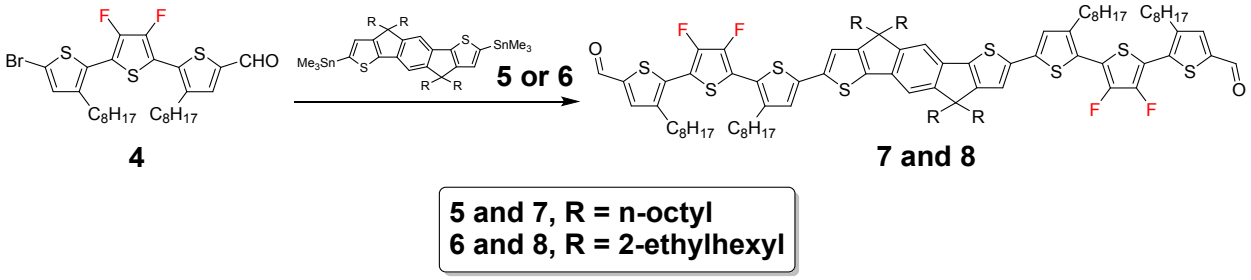

General procedure for the preparation of the aldehyde 7 and 8: In a pre-dried Schlenk tube, aldehyde **4** (2.4 equiv.), organotin reagents **5** or **6** (1.0 equiv.), and $Pd(PPh_3)_4$ (0.08 equiv.) were dissolved with degassed toluene (≈ 50 mL). The mixture was heated at 110 °C for 48 h. The reaction mixture was cooled down to room temperature and concentrated under reduced pressure. The crude product was purified by column chromatography over SiO_2 using hexane/CH_2Cl_2 (1:1) as eluent. The solvent was removed by rotary evaporation, affording compound **7** or **8** as red solid.

Aldehyde 7: ^{1}H NMR (600 MHz, $CDCl_3$, δ ppm): 9.91 (s, 2H), 7.67 (s, 2H), 7.26 (s, 2H), 7.12 (m, 2H), 2.81 (t, J = 7.8 Hz, 4H), 2.76 (t, J = 7.8 Hz, 4H), 2.03-1.99 (m, 4H), 2.03-1.99 (m, 4H), 1.93-1.88 (m, 4H), 1.74-1.69 (m, 8H), 1.43-1.15 (m, 88H), 0.92-0.89 (m, 12H), 0.85-0.83 (m, 12H). ^{13}C NMR (150 MHz, $CDCl_3$, δ ppm): 182.64, 156.05, 153.20, 143.76, (143.31, 143.18, 141.54, 141.40), 142.98, 142.68, (142.29, 142.16, 140.54, 140.41), 139.69, 137.91, 137.87,

135.69, 134.45, 125.16, 121.60, 118.78, (115.11, 115.05, 111.52, 111.47), 113.10, 54.21, 39.13, 31.91, 31.84, 30.50, 30.31, 30.02, 29.67, 29.58, 29.47, 29.44, 29.39, 29.33, 29.27, 29.24, 24.19, 22.69, 22.64, 14.12, 14.10. ^{19}F NMR (564 MHz, $CDCl_3$, δ ppm): (-129.48, -129.51), (-132.68, -132.70). HRMS (+APCI, m/z): calcd. for $C_{106}H_{146}F_4O_2S_8$ $[M+H]^+$: 1783.90974, found 1783.90958.

Aldehyde 8: ^{1}H NMR (400 MHz, $CDCl_3$, δ ppm): 9.91 (s, 2H), 7.67 (s, 2H), 7.30 (s, 2H), 7.14-7.12 (m, 2H), 7.10-7.09(m, 2H), 2.81-2.71 (m, 8H), 1.98 (br, 8H), 1.75-1.67 (m, 8H), 1.41-1.30 (m, 44H), 1.05-0.89 (m, 44H), 0.79-0.52 (m, 24H). ^{13}C NMR (100 MHz, $CDCl_3$, δ ppm): 182.08, 155.28, 152.48, (143.23, 140.95), 142.92, 142.43, 142.27, (142.00, 139.90), 141.39, 139.34, 137.52, 136.99, 135.34, 133.99, 124.72, 121.27, 119.13, 114.69, 113.61, 111.07, 53.63, 43.13, 34.59, 34.56, 33.92, 33.83, 33.46, 33.31, 31.56, 31.53, 30.09, 29.95, 29.34, 29.23, 29.13, 29.08, 29.04, 28.92, 28.35, 28.20, 27.78, 27.10, 26.95, 26.85, 26.65, 22.56, 22.52, 22.46, 22.36, 13.88, 13.78, 10.44, 10.29, 10.06, 10.00, 9.97. ^{19}F NMR (376 MHz, $CDCl_3$, δ ppm): (-129.49, -129.52), (-132.68, -132.72). HRMS (+APCI, m/z): calcd. for $C_{106}H_{146}F_4O_2S_8$ $[M+H]^+$: 1783.90974, found 1783.90983.

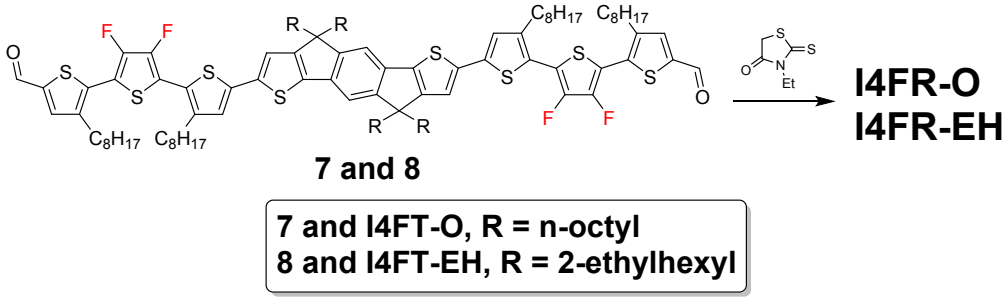

General procedure for the preparation of the donor materials I4FR-O and I4FR-EH: The aldehyde **7** or **8** (1.0 equiv.), 3-ethylrhodanine (10.0 equiv.) and basic Al_2O_3 (5.0 equiv.) were added into a solution of anhydrous chloroform (20 mL), and the mixture was heated to 70 °C and stirred for 24 h. The reaction mixture was allowed to cool down to room temperature, was filtered, was washed with chloroform (2 × 30 mL), and was concentrated under reduced pressure. The crude product was purified by column chromatography over SiO_2 using chloroform/hexanes (2:1) as the eluent. The solvent was removed by rotary evaporation, affording the desired products (**I4FR-O** or **I4FR-EH**) as purple-bluish solid.

I4FR-O: ^{1}H NMR (600 MHz, CD_2Cl_2, δ ppm): 7.86, 7.36, 7.36, 7.19, 7.18, 4.23-4.19 (m, 4H), 2.84-2.77 (m, 8H), 2.08-2.04 (m, 4H), 1.97-1.94 (m, 4H), 1.77-1.70 (m, 8H), 1.46-1.16 (m, 94), 0.93-0.91 (m, 12H), 0.86-0.84 (m, 12H). ^{13}C NMR (150 MHz, $CDCl_3$, δ ppm): 191.93, 167.24, 156.07, 153.22, 143.70, 143.63, (143.05, 142.92, 141.28, 141.15), (142.37, 142.23, 140.61, 140.48), 141.49, 139.65, 137.92, 137.76, 135.90, 135.72, 132.49, 125.18, 124.38, 121.83, 118.77, (114.75, 114.66, 111.72, 111.64), 113.11, 54.23, 39.95, 39.11, 31.88, 31.85, 31.81, 30.45, 30.32, 30.00, 29.67, 29.55, 29.48, 29.42, 29.36, 29.29, 29.24, 29.22, 24.19, 22.66, 22.65, 22.60, 14.07, 14.03, 12.25. ^{19}F NMR (564 MHz, $CDCl_3$, δ ppm): (-129.99, -130.01), (-132.67, -132.70). HRMS (+APCI, m/z): calcd. for $C_{116}H_{156}F_4N_2O_2S_{12}$ $[M+H]^+$: 2069.88242, found 2069.88261.

I4FR-EH: ^{1}H NMR (400 MHz, CD_2Cl_2, δ ppm): 7.86 (s, 2H), 7.39 (s, 2H), 7.36 (s, 2H), 7.21-7.20 (m, 2H), 7.16 (m, 2H), 4.24-4.18 (m, 4H), 2.84-2.76 (m, 8H), 2.03 (br, 8H), 1.75-1.68 (m, 8H), 1.44-1.29 (m, 50), 1.06-0.90 (m, 44H), 0.81-0.55 (m, 24H). ^{13}C NMR (100 MHz, $CDCl_3$, δ ppm): 191.95, 167.25, 155.78, 152.91, 143.64, 143.05, 142.94, 141.77, 141.28, 140.58, 139.72, 137.75, 135.92, 135.73, 132.52, 125.14, 124.40, 121.80, 119.60, 114.78, 114.00, 111.69, 54.04, 44.07, 43.64, 39.96, 35.08, 35.05, 35.00, 34.31, 34.22, 33.91, 33.78, 31.88, 31.85, 30.42, 30.32, 29.67, 29.55, 29.47, 29.41, 29.35, 29.23, 29.21, 28.73, 28.61, 28.19, 27.41, 27.27, 27.21, 27.01, 22.90, 22.86, 22.81, 22.66, 22.65, 14.16, 14.07, 12.25, 10.74, 10.61, 10.36, 10.34, 10.29. ^{19}F NMR (376 MHz, $CDCl_3$, δ ppm): (-131.26, -131.29), (-133.75, -133.78). HRMS (+APCI, m/z): calcd. for $C_{116}H_{156}F_4N_2O_2S_{12}$ $[M+H]^+$: 2069.88242, found 2069.88230.

3. Density Functional Theory (DFT) Calculations

The frontier molecular orbital of the these two compounds at the B3LYP/6-31G level are presented in **Figure 5**, the surfaces are generated with an isovalue of 0.02. As **Figure 5** shows, the electron density is uniformly distributed along the IDT unit and adjacent thiophene linkers at the HOMO state. At the LUMO level the excited electrons are shifted to the π-electron system of the π-linker and anchoring group, which can be assigned to the ICT along the π-conjugated skeleton. By checking the computationally optimized structures.

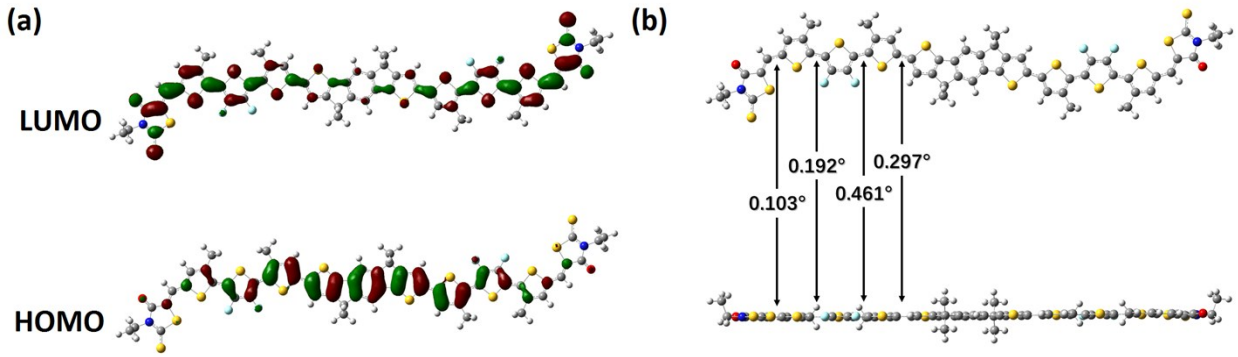

Figure S1. Ball and stick model of the fully optimized ground-state geometries for **I4FR-O** and **I4FR-EH**.

4. Photoelectron Spectroscopy in Air (PESA) Measurements

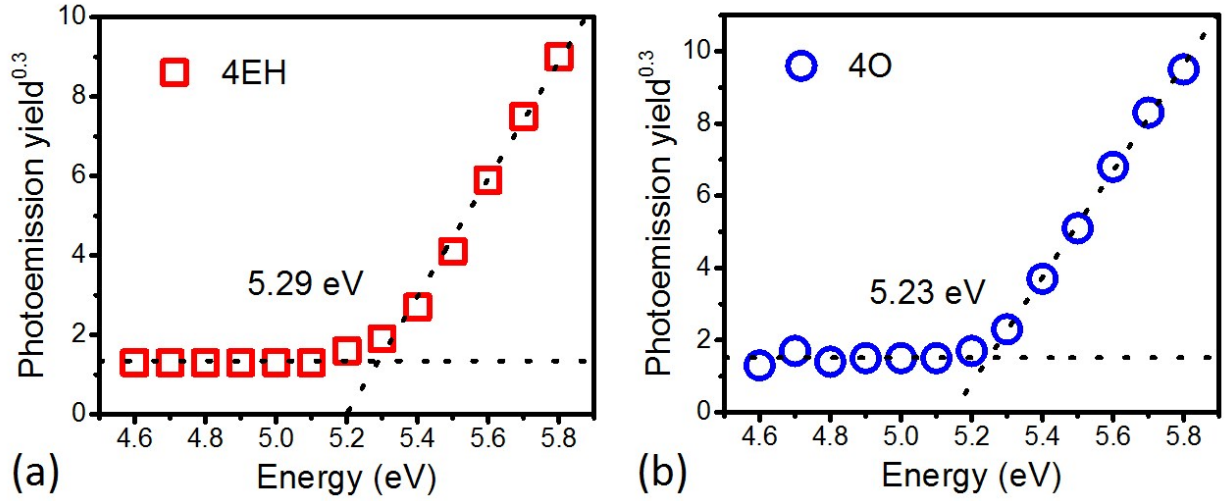

Figure S2. PESA curves for **D5T6F-M** and **D7T8F-M**; PESA-inferred ionization potentials (IPs) are reported on the plots.

5. Internal Quantum Efficiency (IQE)

The internal quantum efficiency (IQE) of the BHJ devices made with SM donor and $PC_{70}BM$ was calculated from **Equation S1**:

$$IQE = EQE / (1\text{-}R\text{-}ParAbs) \quad (\mathbf{S1})$$

The EQE spectra were collected from optimized BHJ devices with the following configuration: Glass/ITO/PEDOT:PSS/SM:$PC_{70}BM$/Ca/Al (details given in Section 4). The reflectance (R) spectra were collected via EQE instrument equipped with an integrating sphere collecting the scattered light. The parasitic absorption (ParAbs) was obtained from transfer matrix modeling.

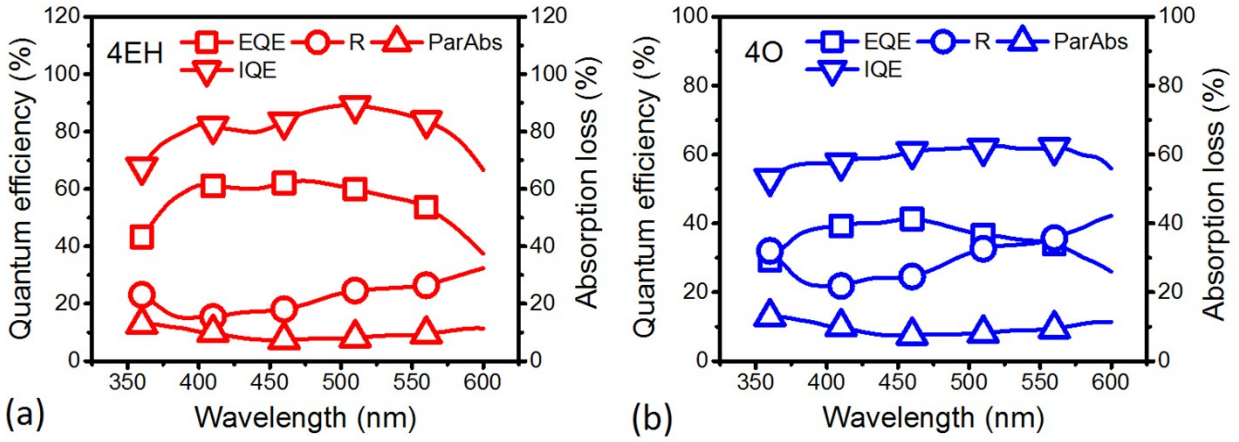

Figure S3. EQE, IQE, reflectance and parasitic absorption of SM:$PC_{70}BM$ BHJ devices.

6. Carrier Mobility Measurements

The carrier mobility (hole and electron mobility) of photoactive active layer was obtained by fitting the dark current of hole/electron-only diodes to the space-charge-limited current (SCLC) model. Hole-only diode configuration: Glass/ITO/PEDOT:PSS/active layer/MoO_3/Ag; here, V_{bi}=0 V (flat band pattern formed by PEDOT:PSS-MoO_3). Electron-only diode configuration: Glass/ITO/ZnO/active layer/Ca/Al; here, V_{bi}=0.5V was used following the protocol reported.[4] The active layer thickness was determined by a Tencor surface profilometer. The electric-field dependent SCLC mobility was estimated using the following equation:

$$J(V) = \frac{9}{8}\varepsilon_0\varepsilon_r\mu_0 exp\left(0.89\beta\sqrt{\frac{V - V_{bi}}{L}}\right)\frac{(V - V_{bi})^2}{L^3}$$

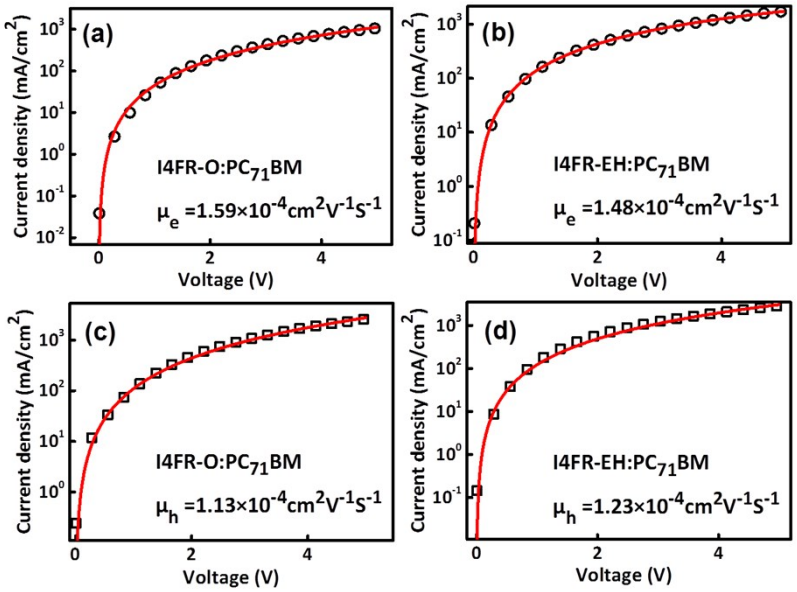

Figure S4. (a,b) the electron mobility fitting examples of I4FR-O and I4FR-EH, respectively; (c,d) the hole mobility fitting examples of I4FR-O and I4FR-EH, respectively.

Table S1. Average mobility values of devices of I4FR-O:$PC_{70}BM$ and I4FR-EH:$PC_{70}BM$.

System	μ_e ($cm^2V^{-1}s^{-1}$)	μ_h ($cm^2V^{-1}s^{-1}$)
I4FR-O:$PC_{70}BM$	1.59×10^{-4}	1.13×10^{-4}
I4FR-EH:$PC_{70}BM$	1.48×10^{-4}	1.23×10^{-4}

7. Solution NMR Spectra

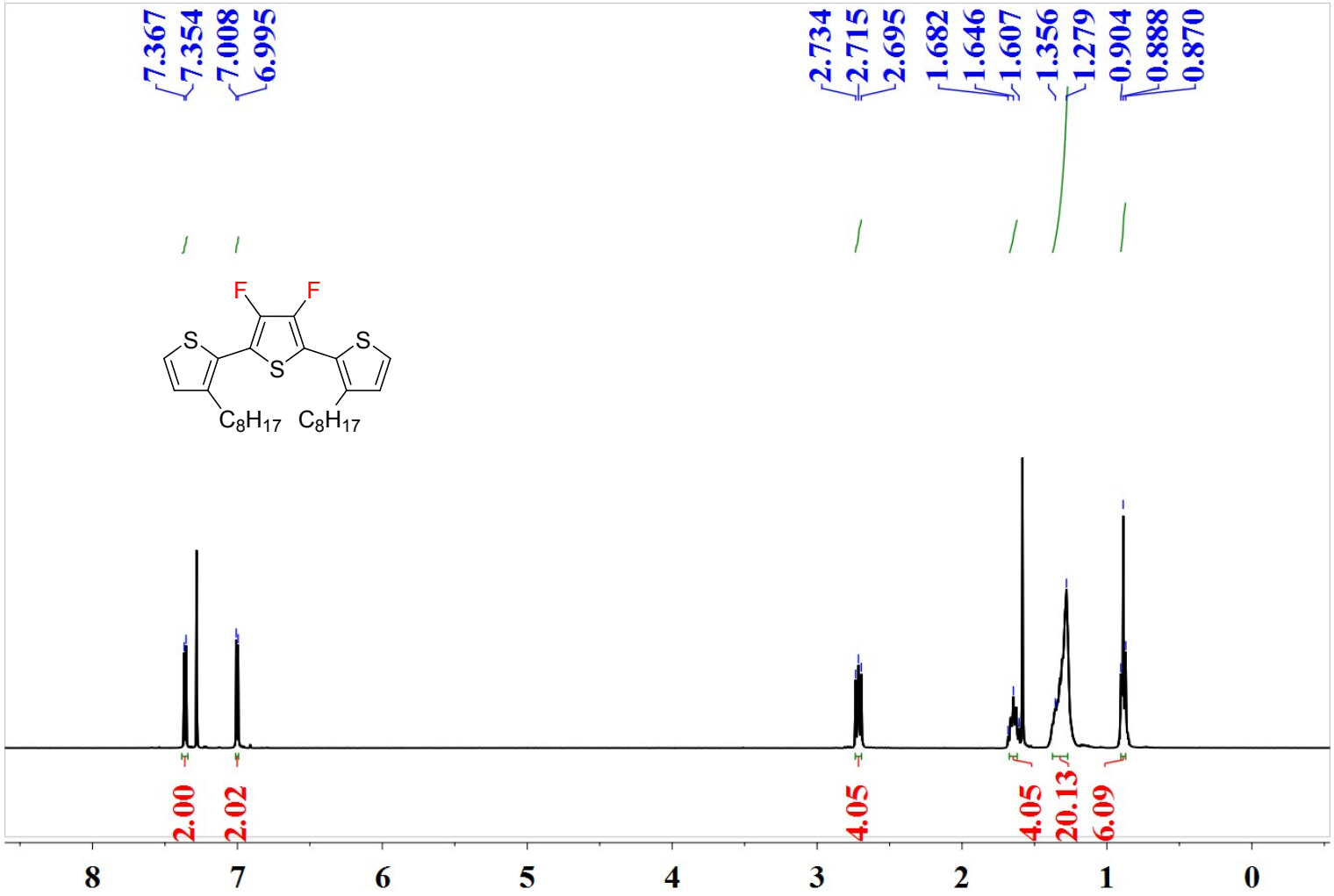

Figure S5. ^{1}H NMR spectrum of **2** in $CDCl_3$.

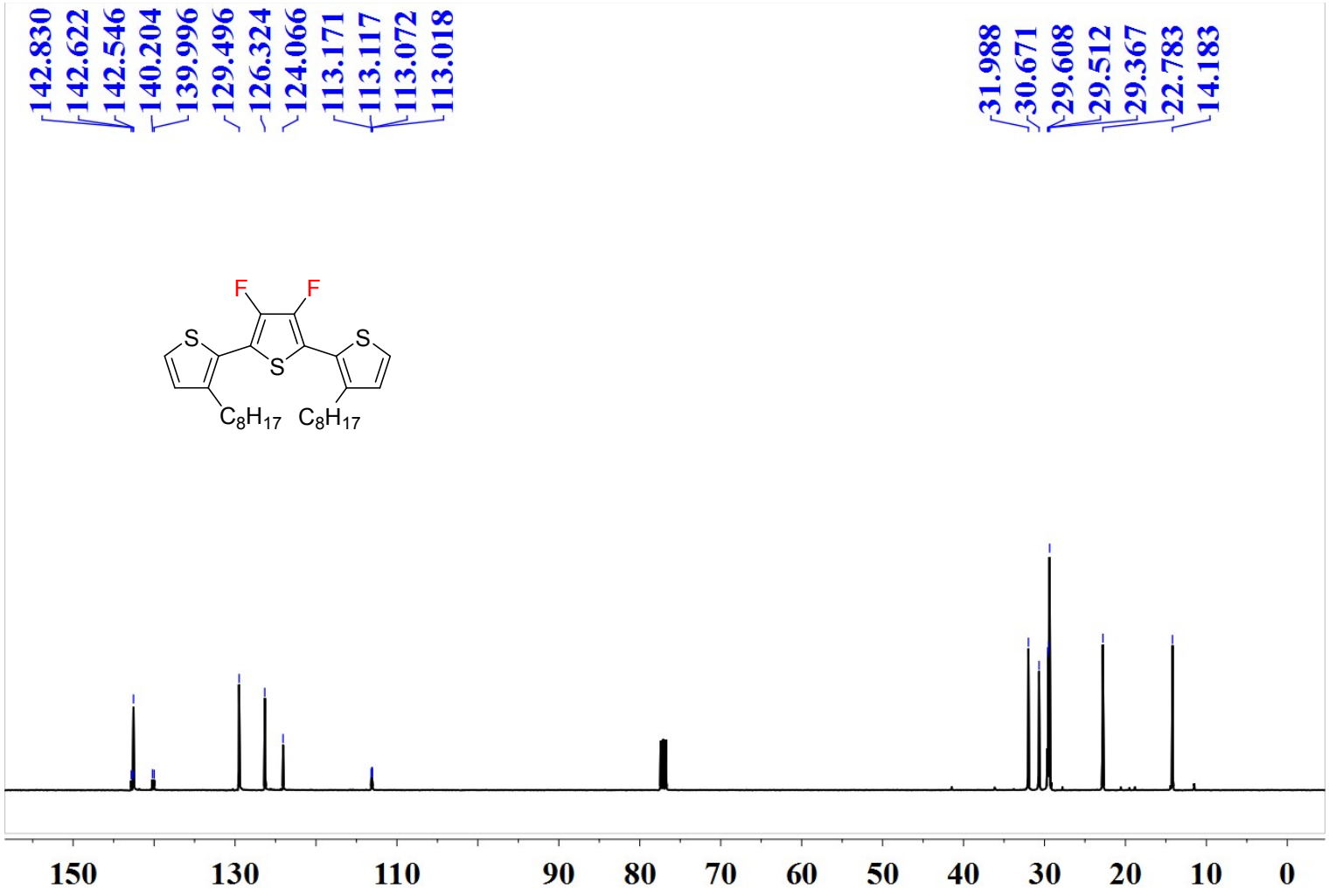

Figure S6. ^{13}C NMR spectrum of **2** in $CDCl_3$.

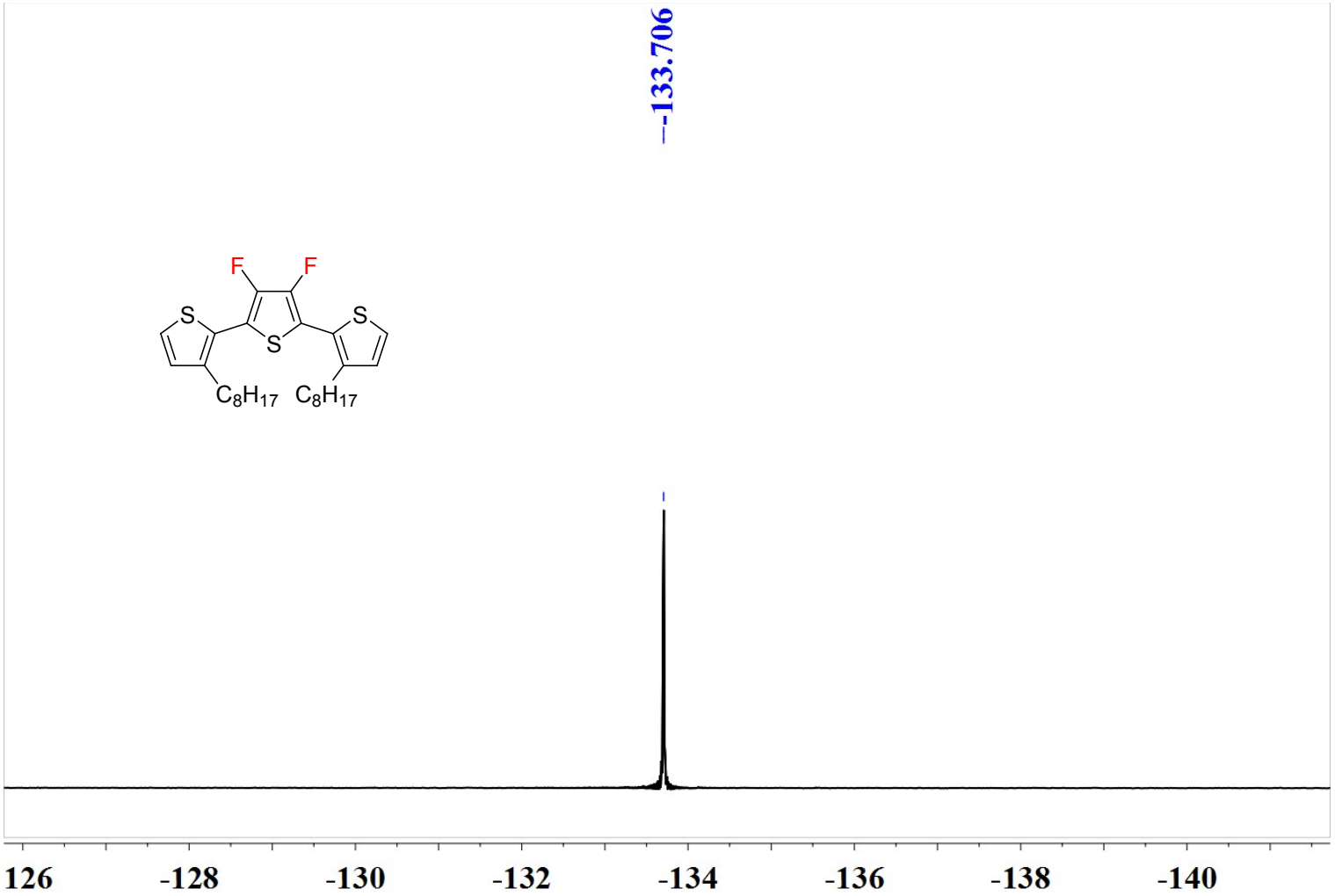

Figure S7. ^{19}F NMR spectrum of **2** in $CDCl_3$.

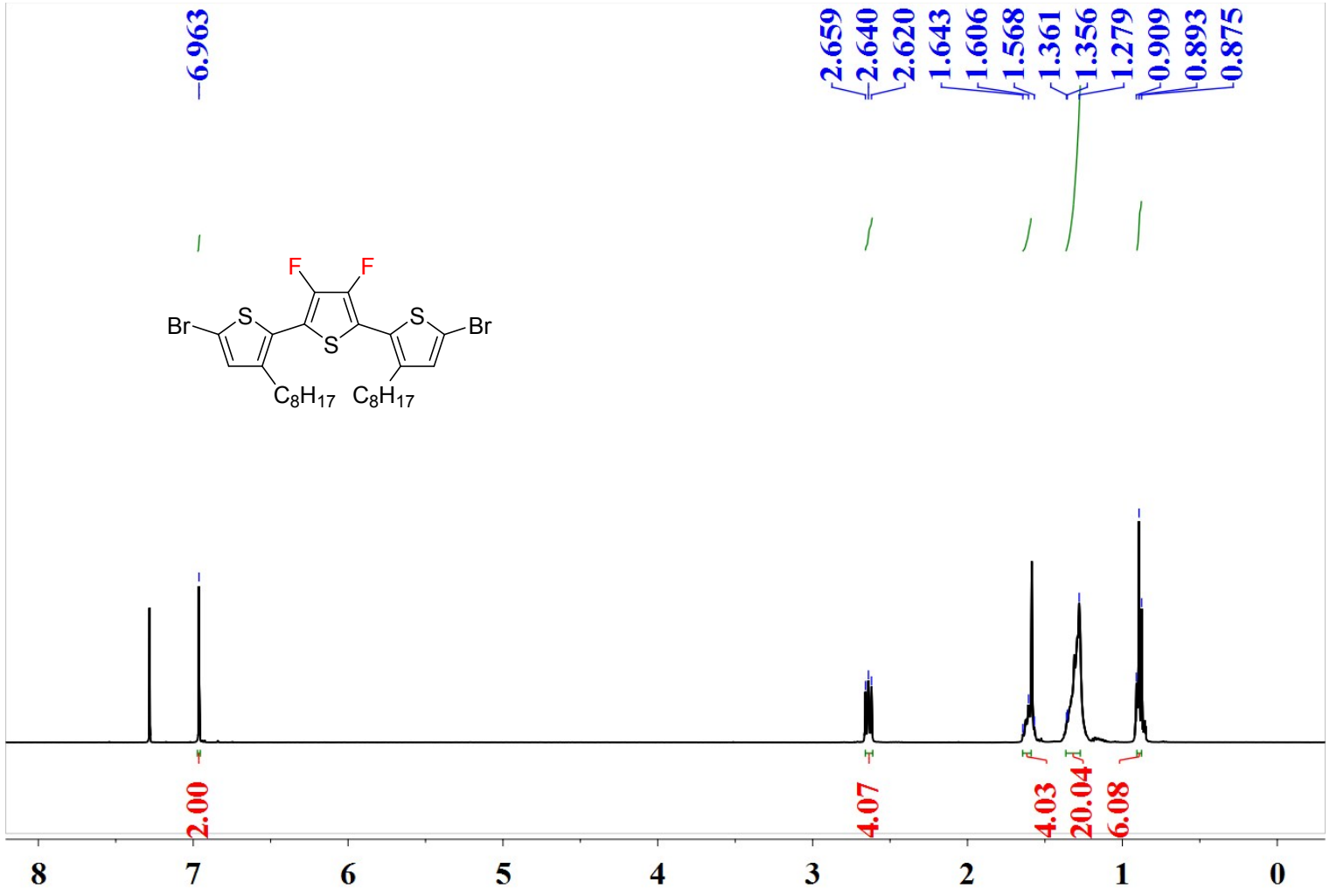

Figure S8. ^{1}H NMR spectrum of **3** in $CDCl_3$.

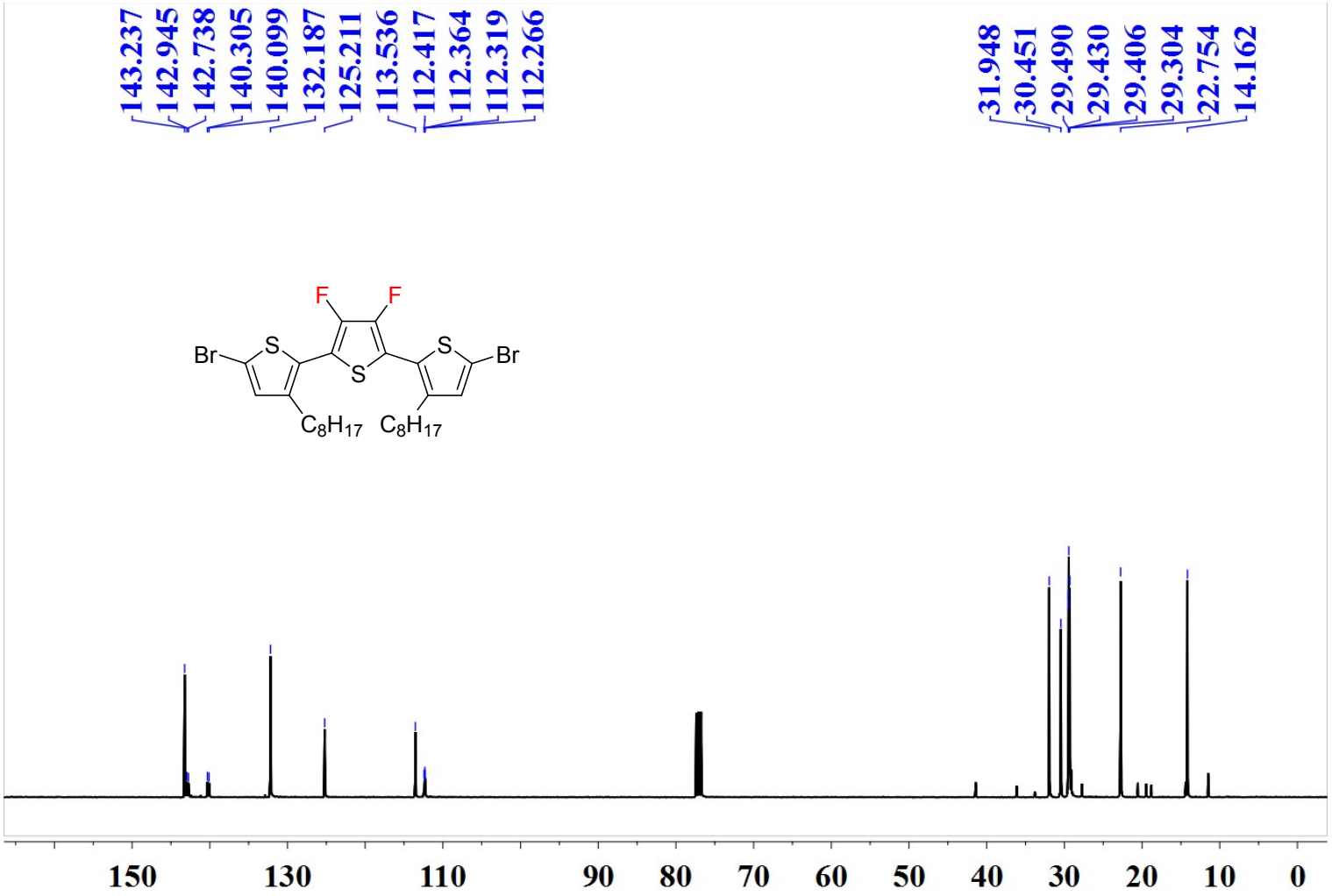

Figure S9. ^{13}C NMR spectrum of **3** in $CDCl_3$.

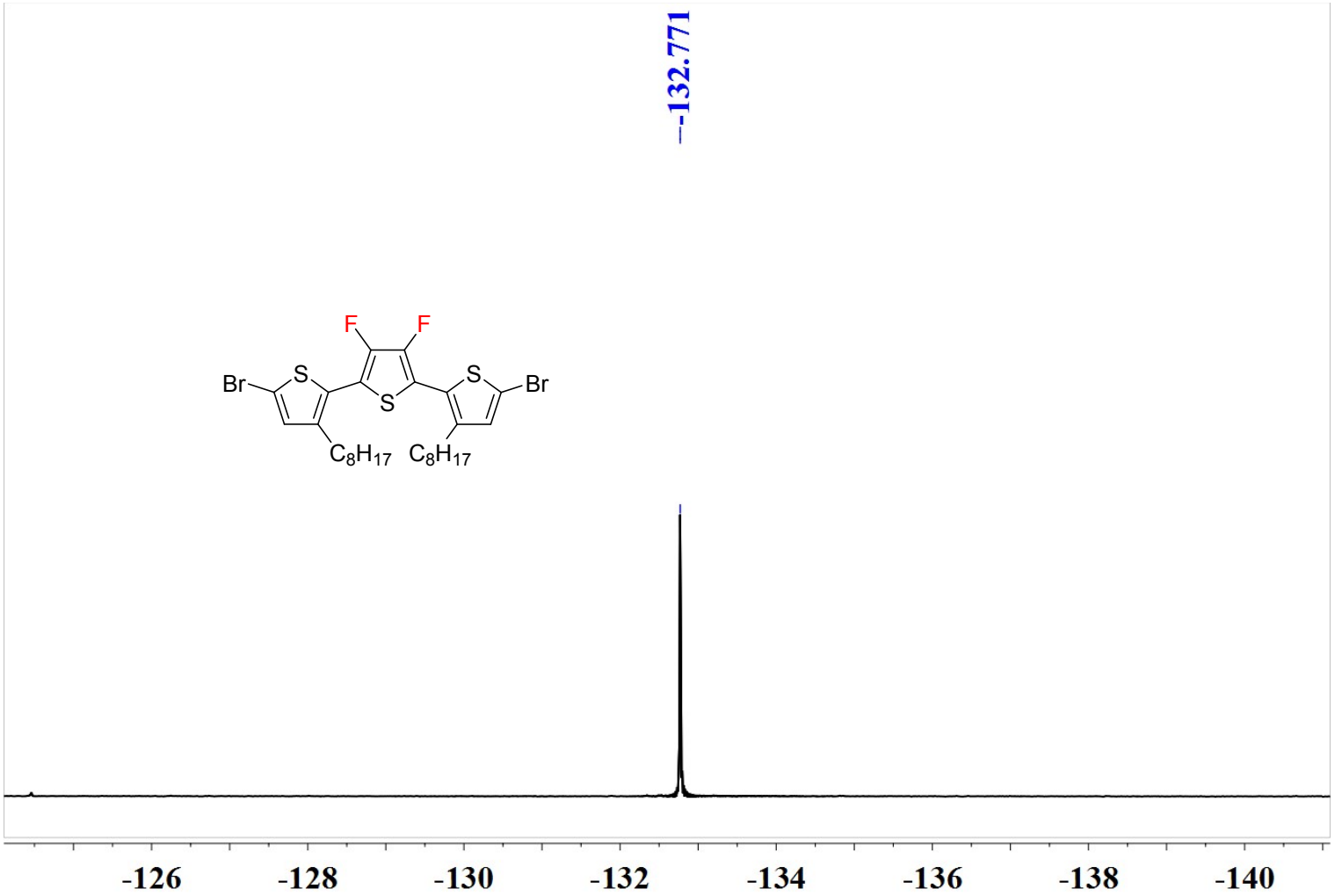

Figure S10. ^{19}F NMR spectrum of **3** in $CDCl_3$.

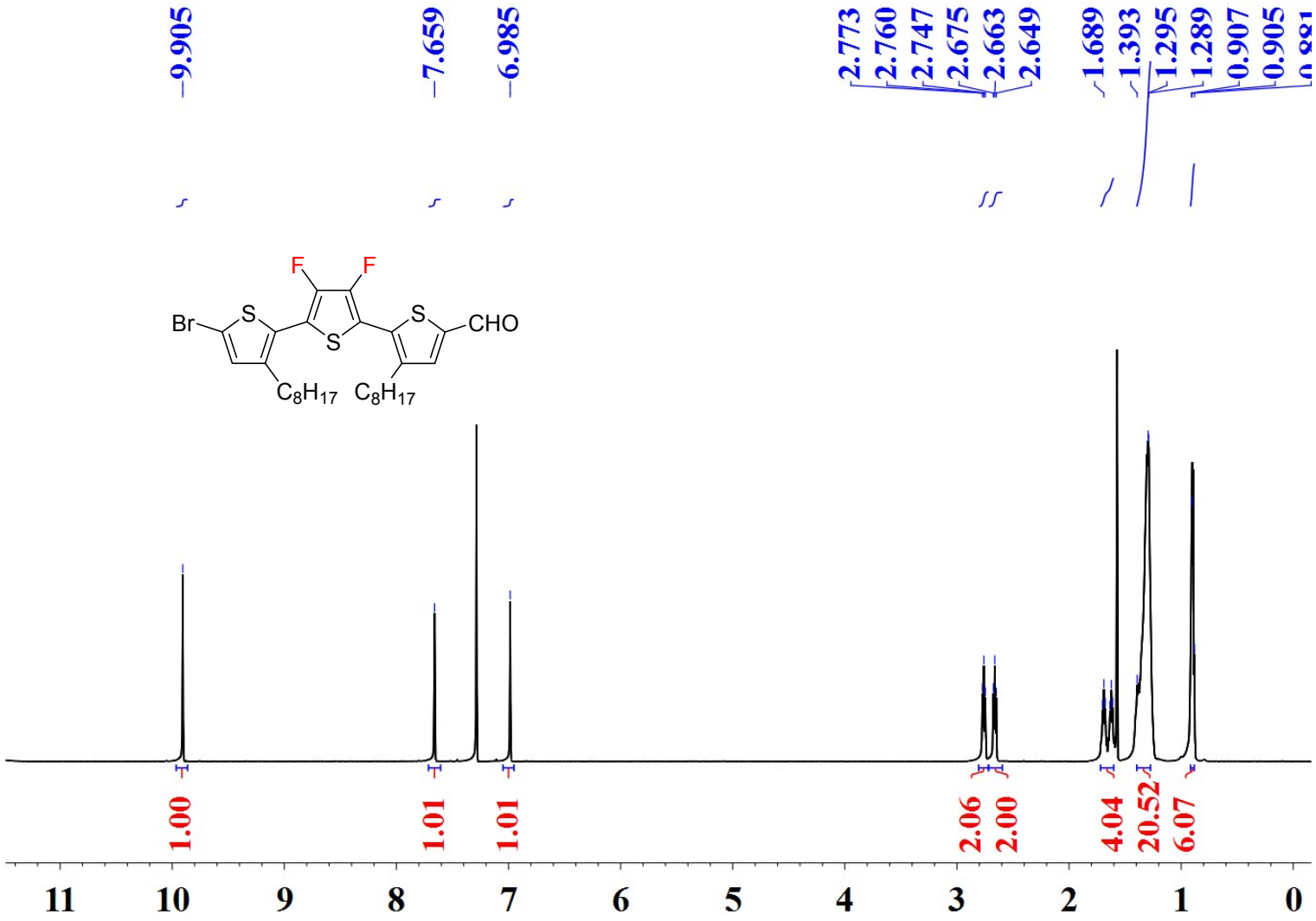

Figure S11. ^{1}H NMR spectrum of **4** in $CDCl_3$.

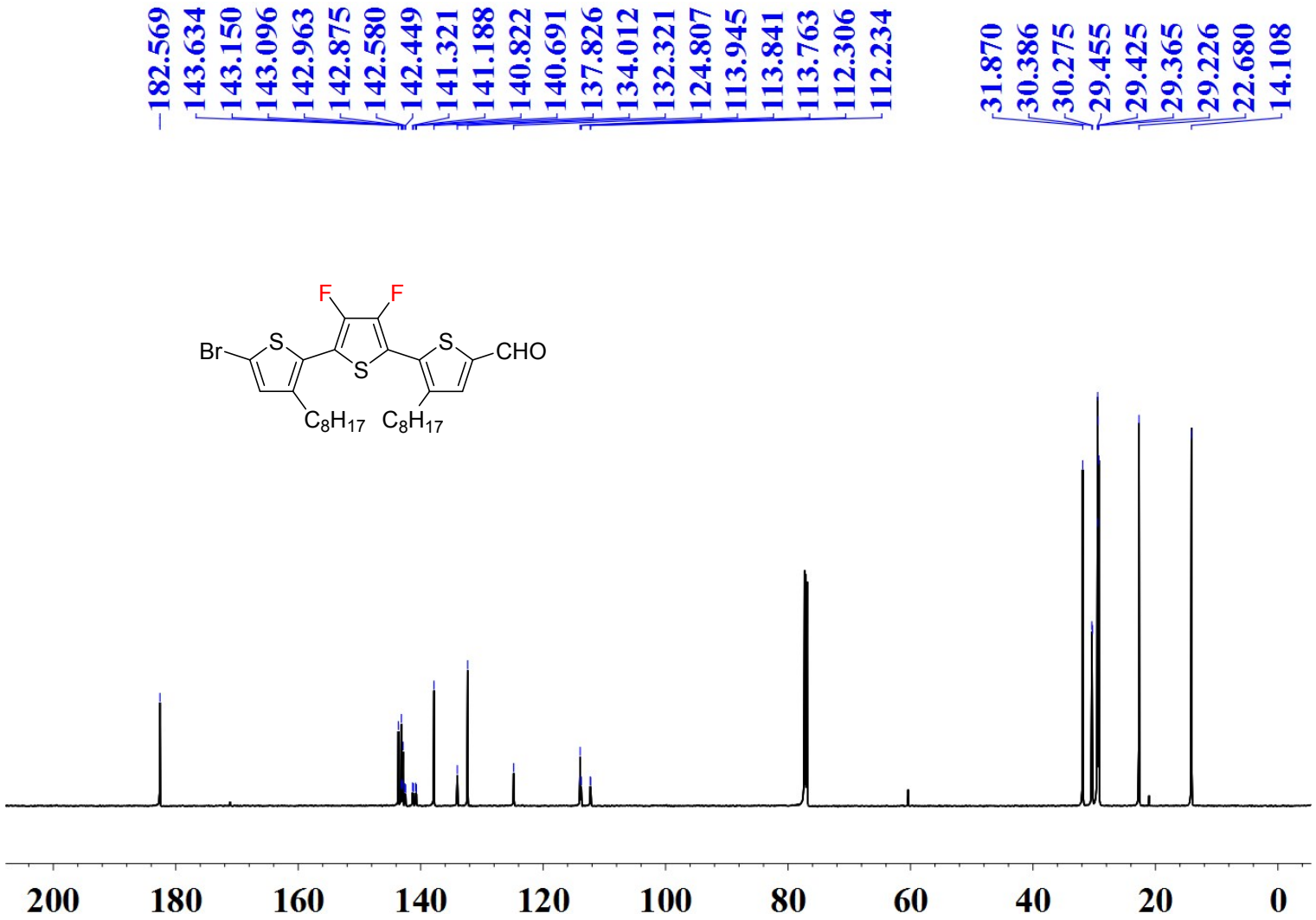

Figure S12. ^{13}C NMR spectrum of **4** in $CDCl_3$.

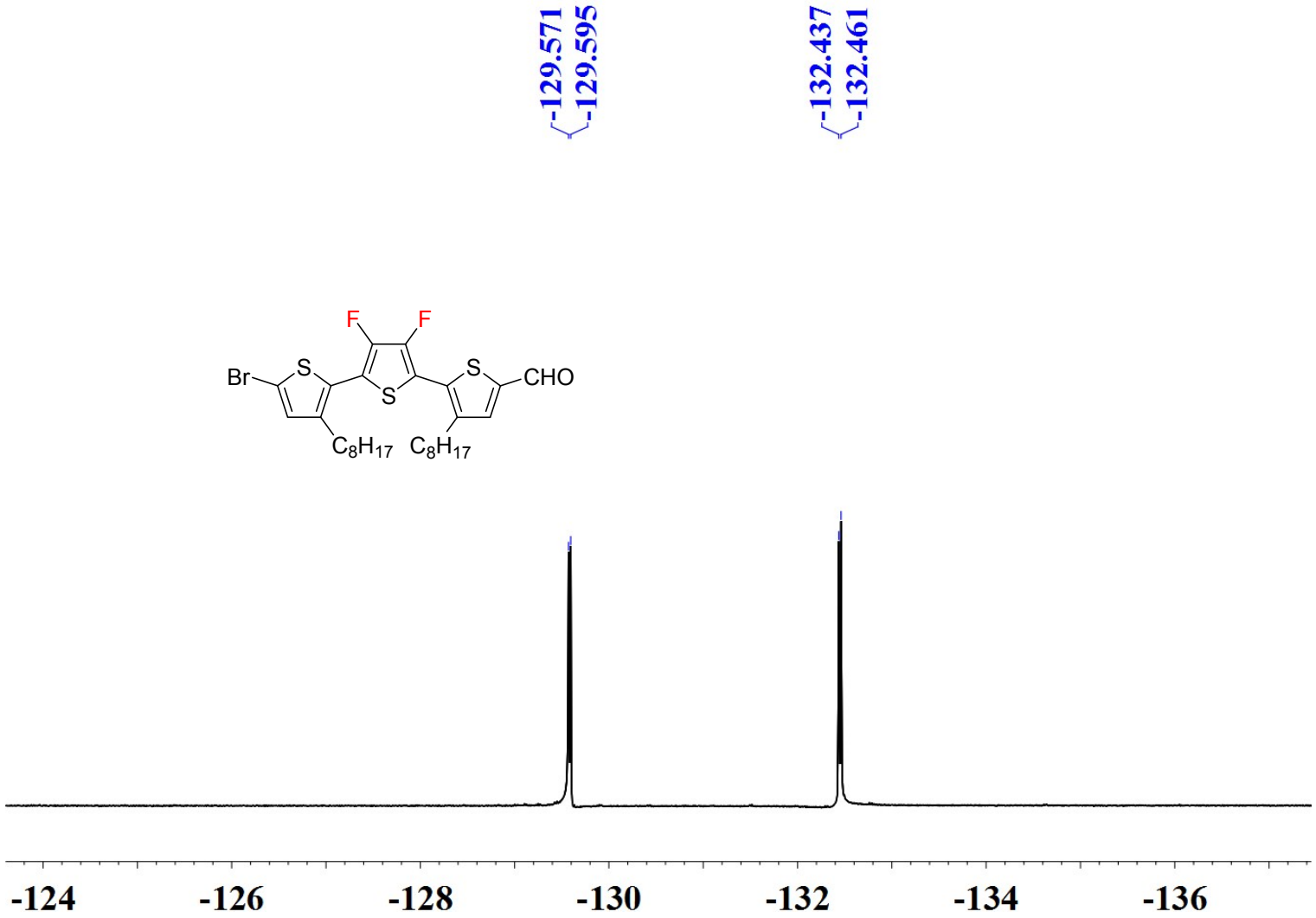

Figure S13. ^{19}F NMR spectrum of **4** in $CDCl_3$.

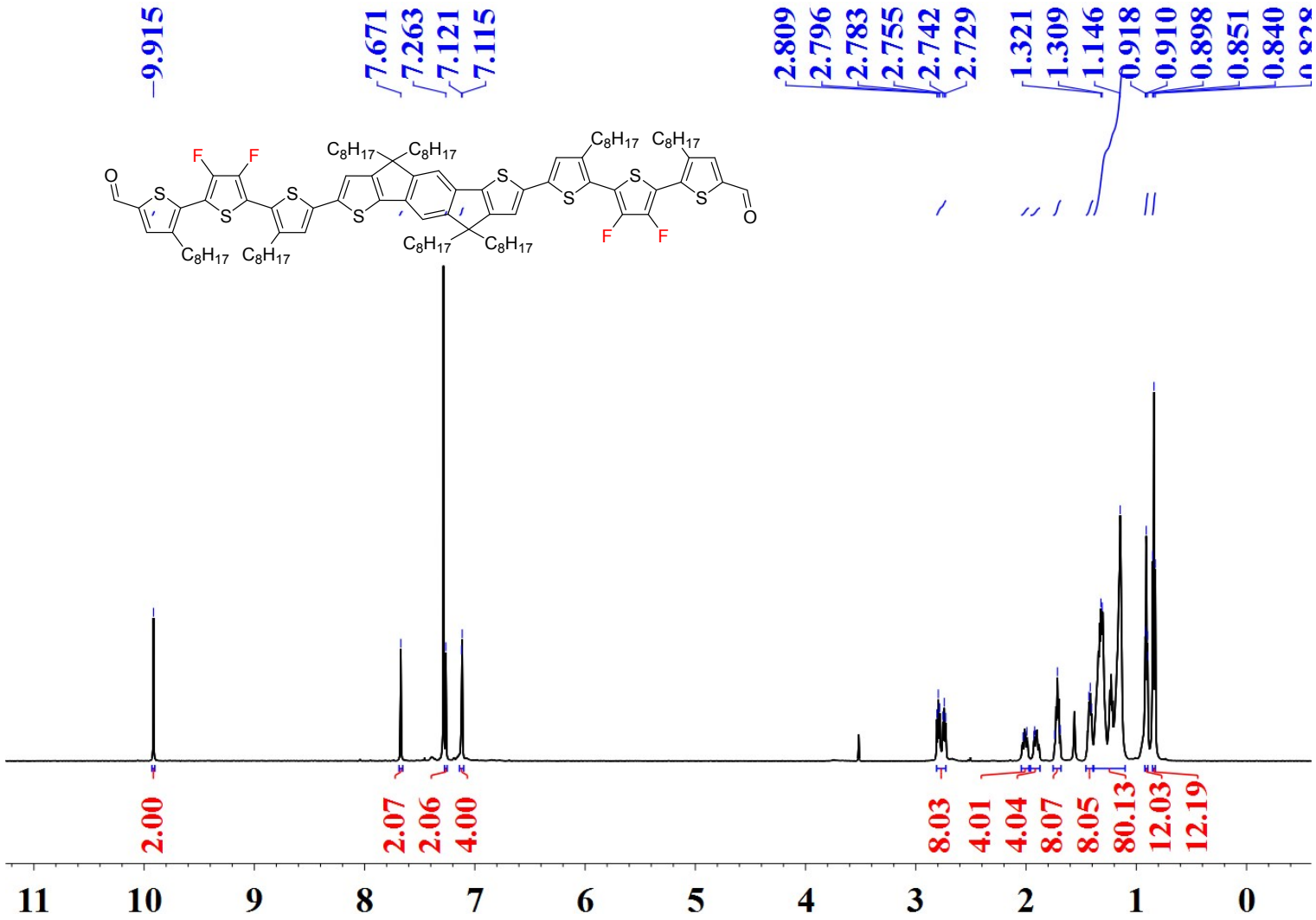

Figure S14. ^{1}H NMR spectrum of **7** in $CDCl_3$.

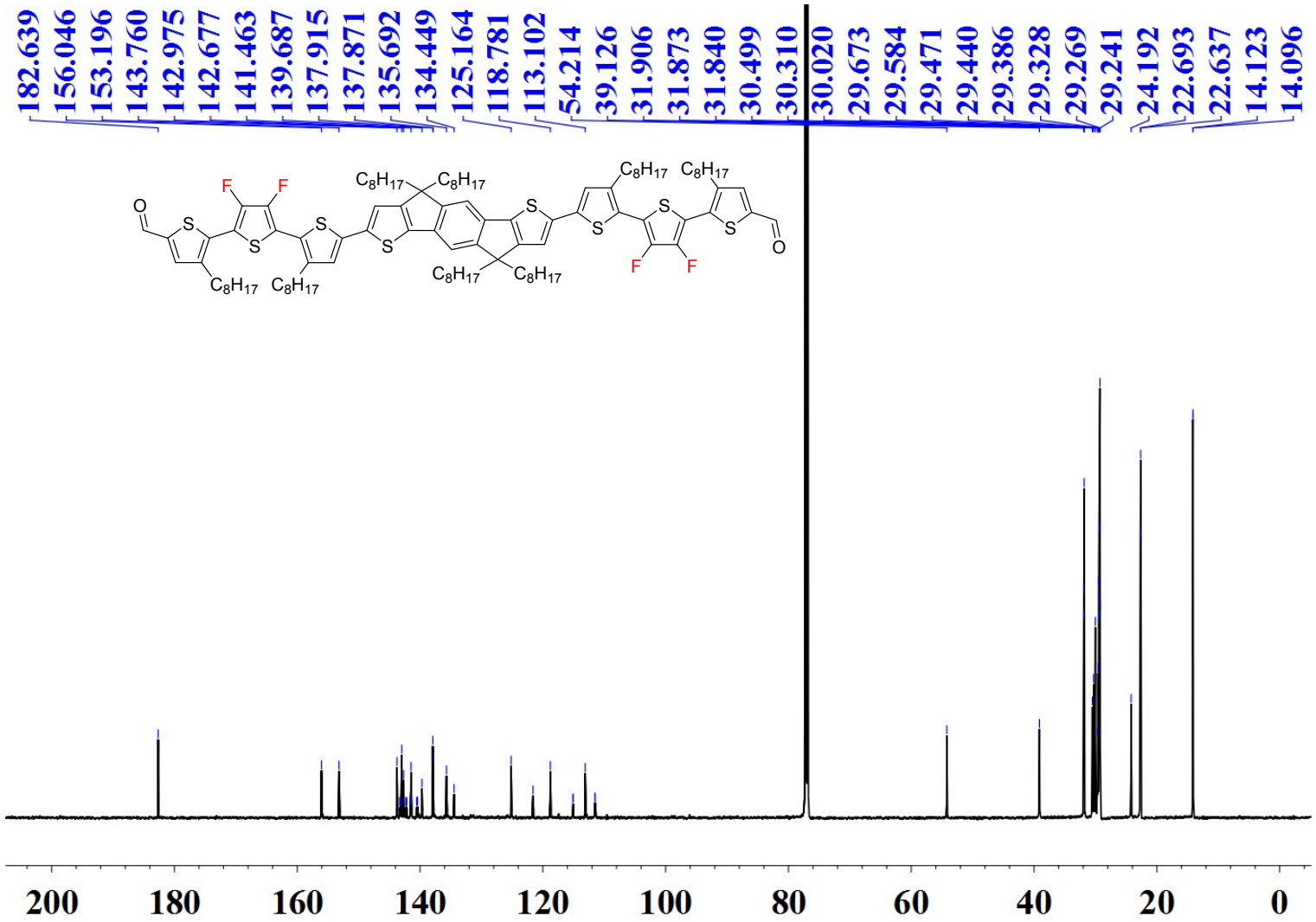

Figure S15. ^{13}C NMR spectrum of **7** in $CDCl_3$.

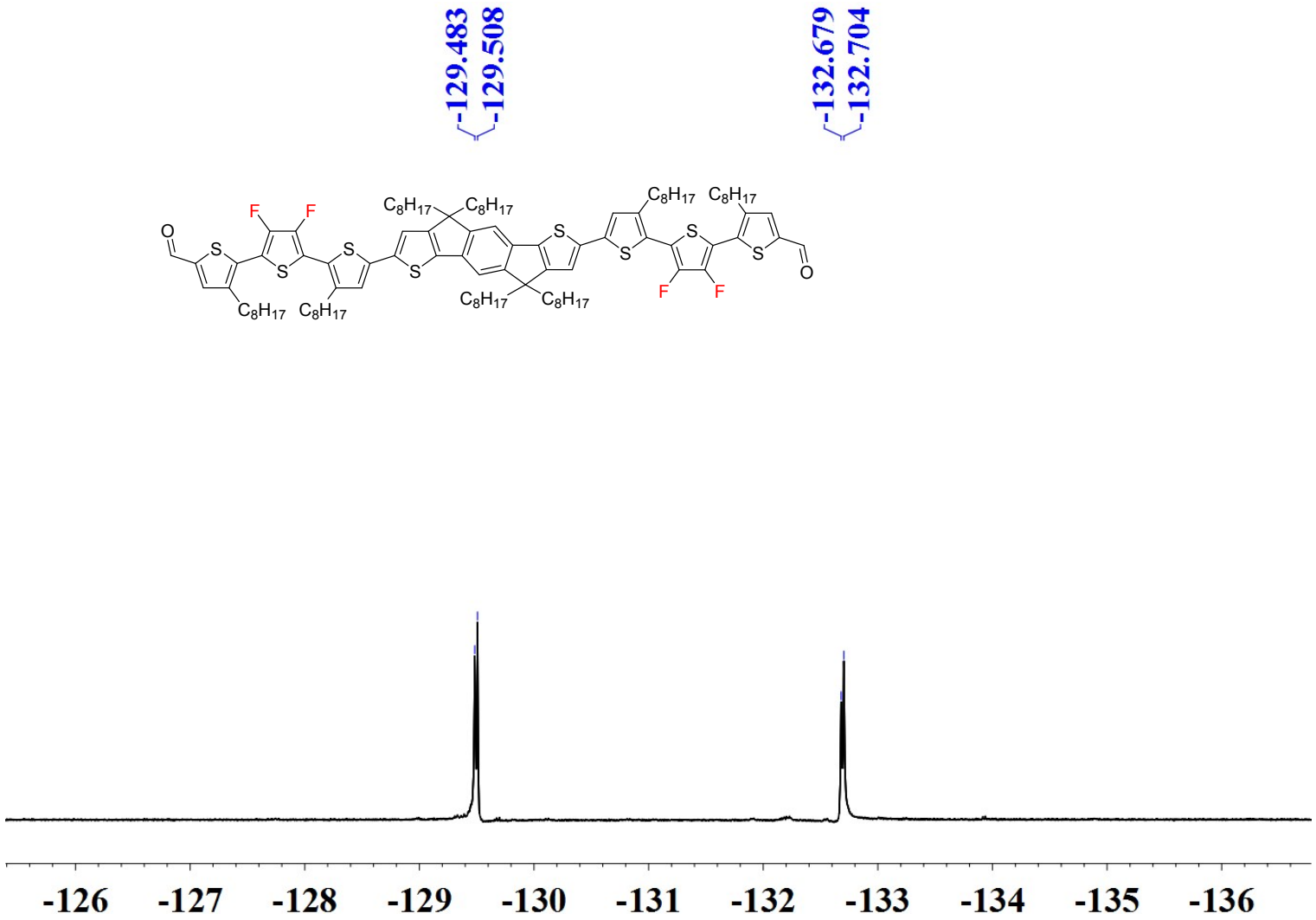

Figure S16. ^{19}F NMR spectrum of **7** in $CDCl_3$.

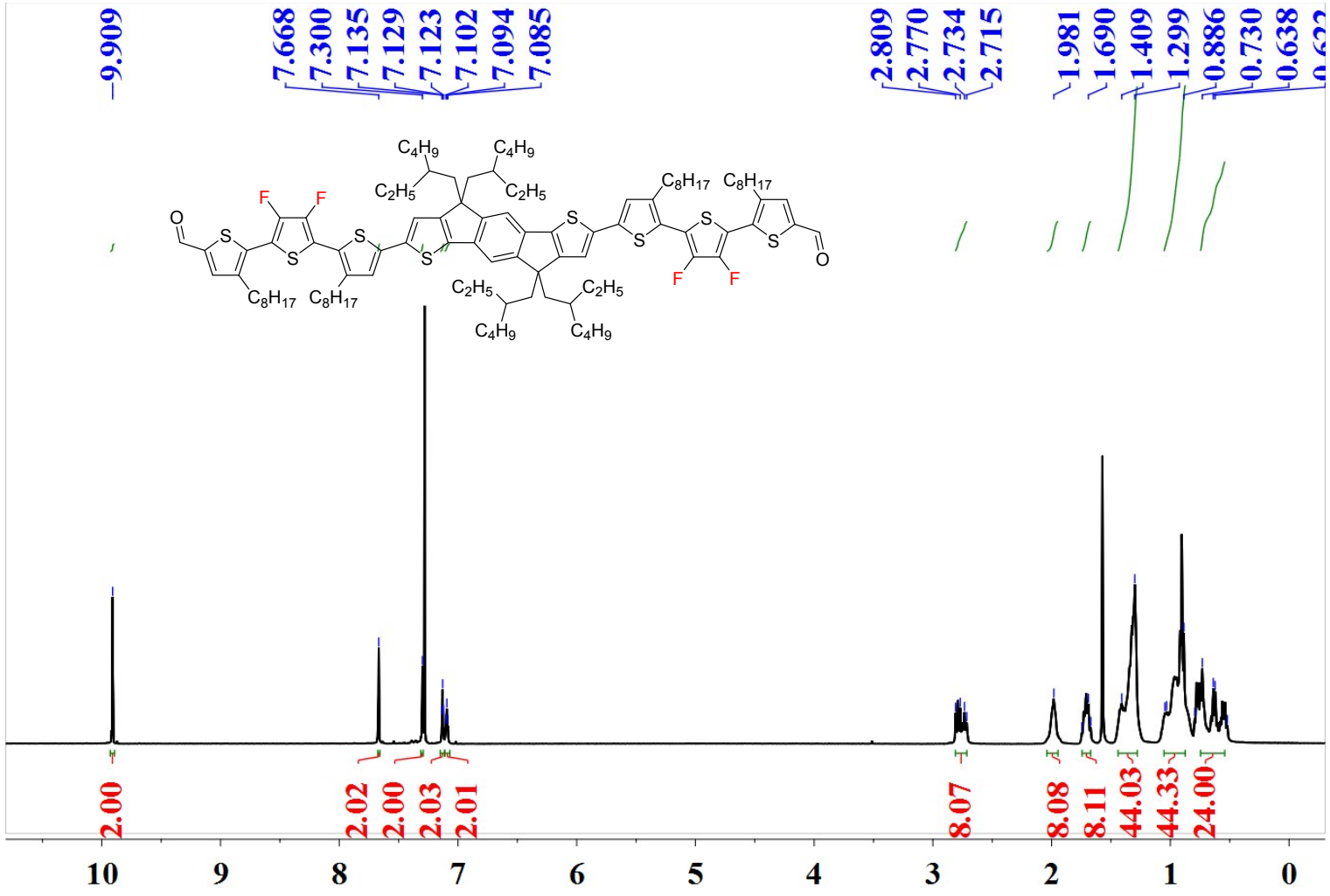

Figure S17. ^{1}H NMR spectrum of **8** in $CDCl_3$.

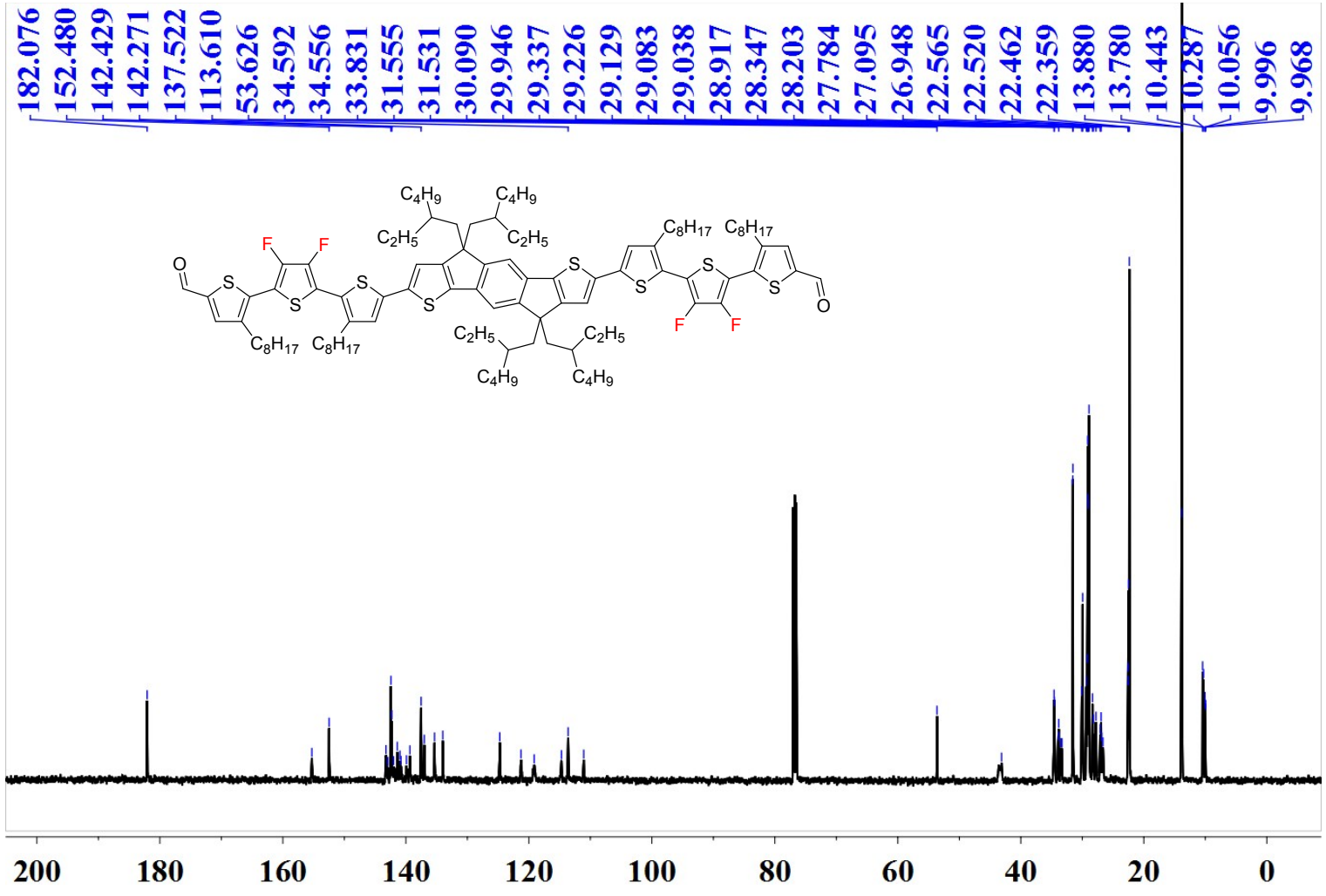

Figure S18. ^{13}C NMR spectrum of **8** in $CDCl_3$.

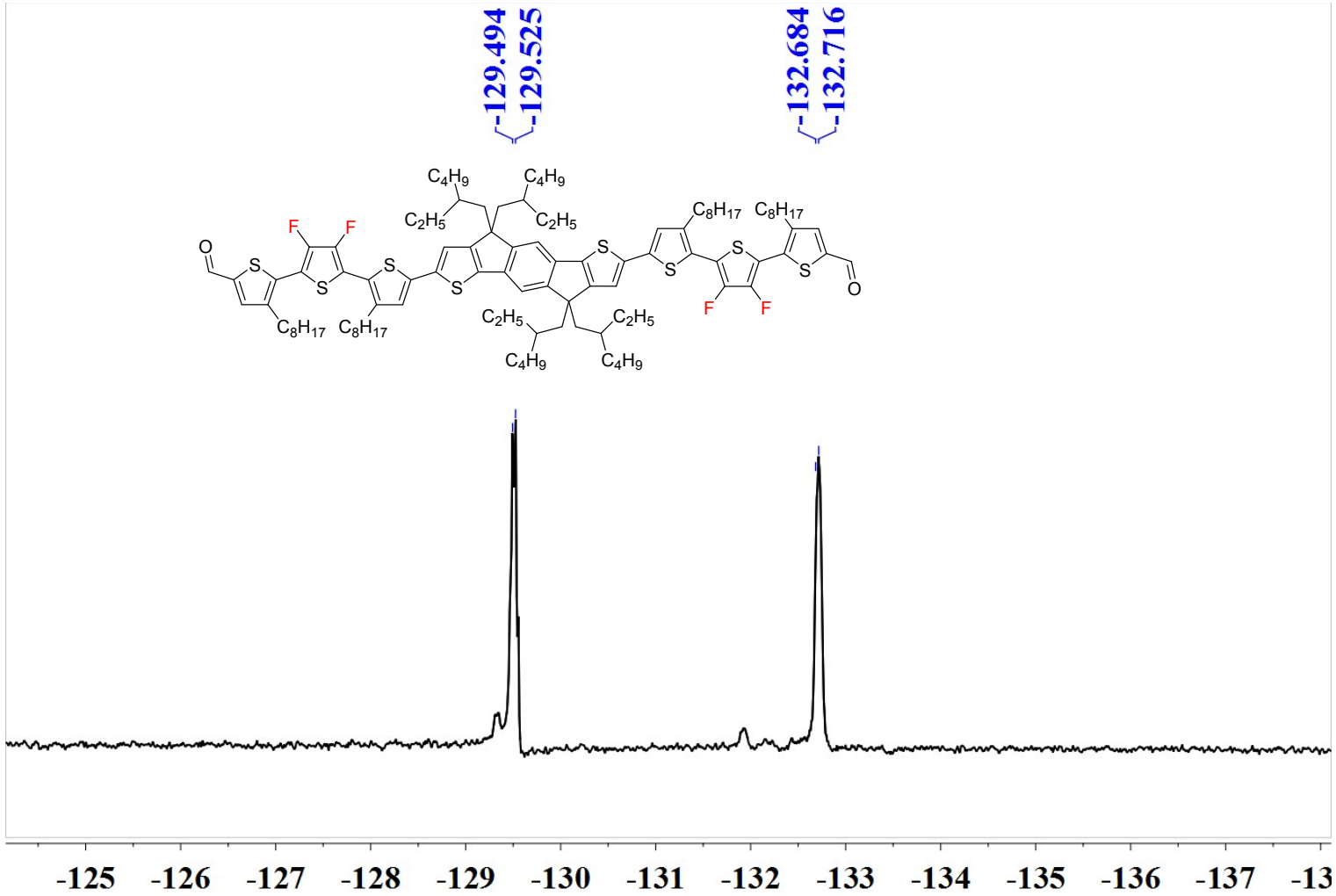

Figure S19. ^{19}F NMR spectrum of **8** in $CDCl_3$.

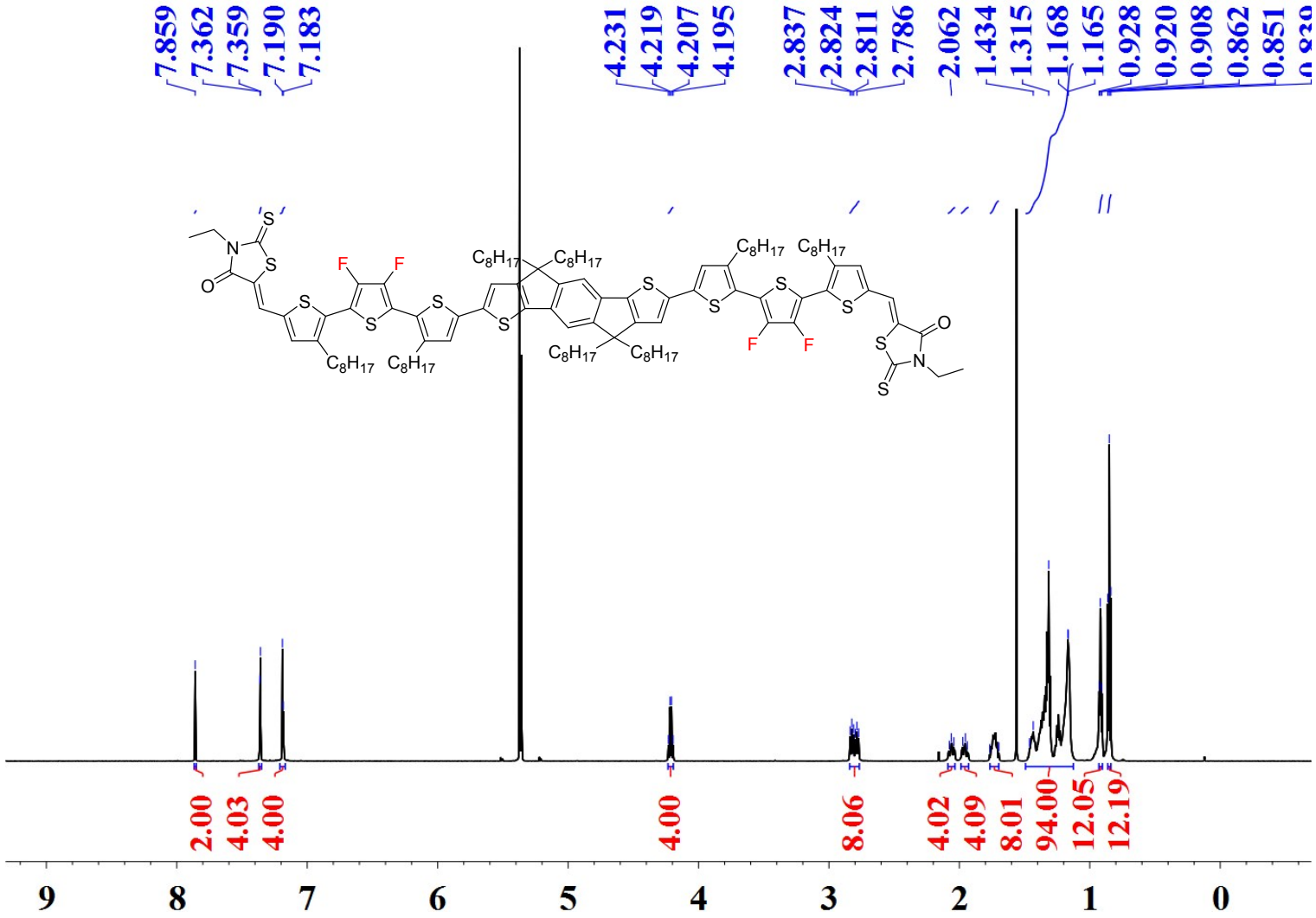

Figure S20. ^{1}H NMR spectrum of **I4FR-O** in CD_2Cl_2.

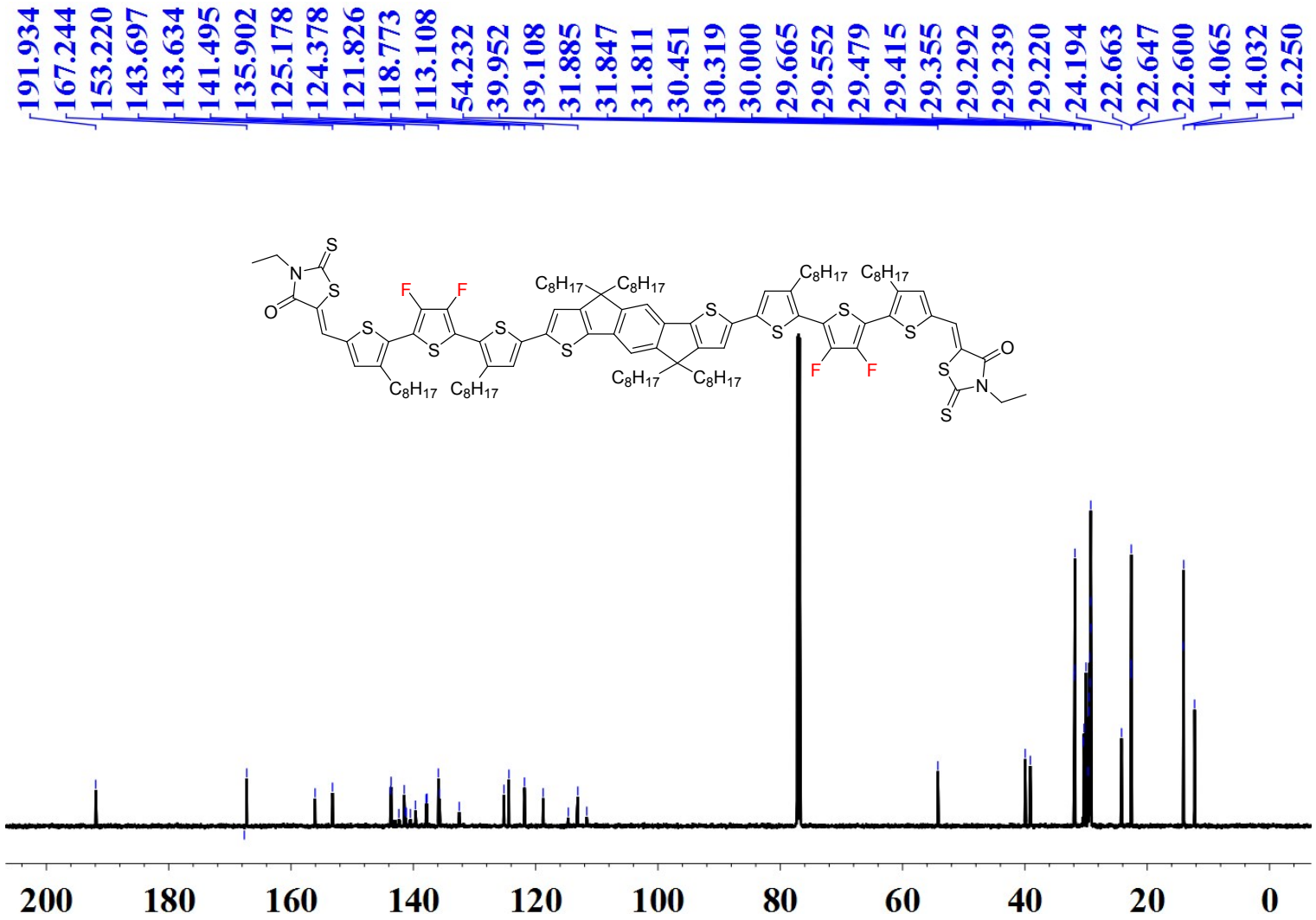

Figure S21. ^{13}C NMR spectrum of **I4FR-O** in $CDCl_3$.

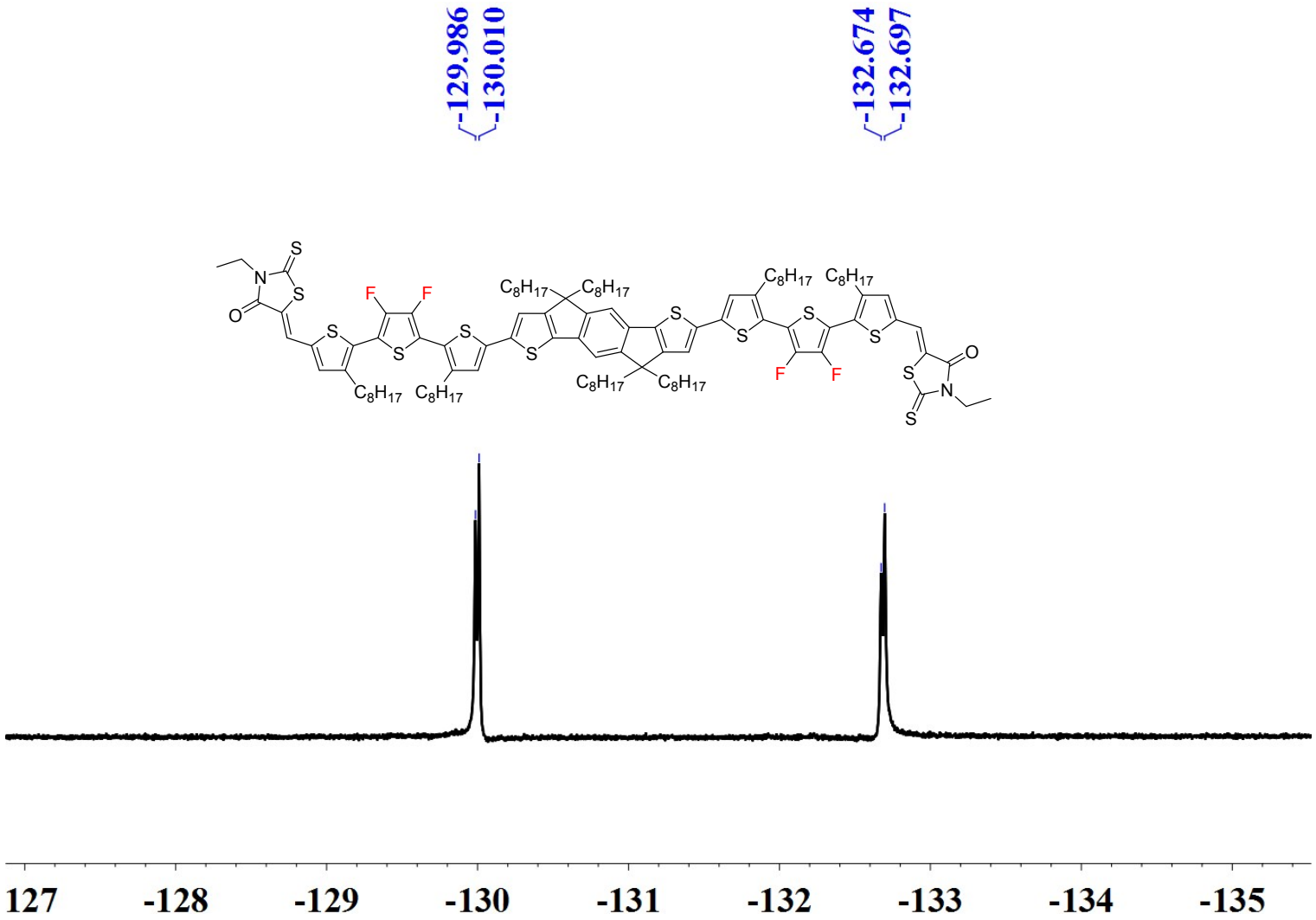

Figure S22. ^{19}F NMR spectrum of **I4FR-O** in $CDCl_3$.

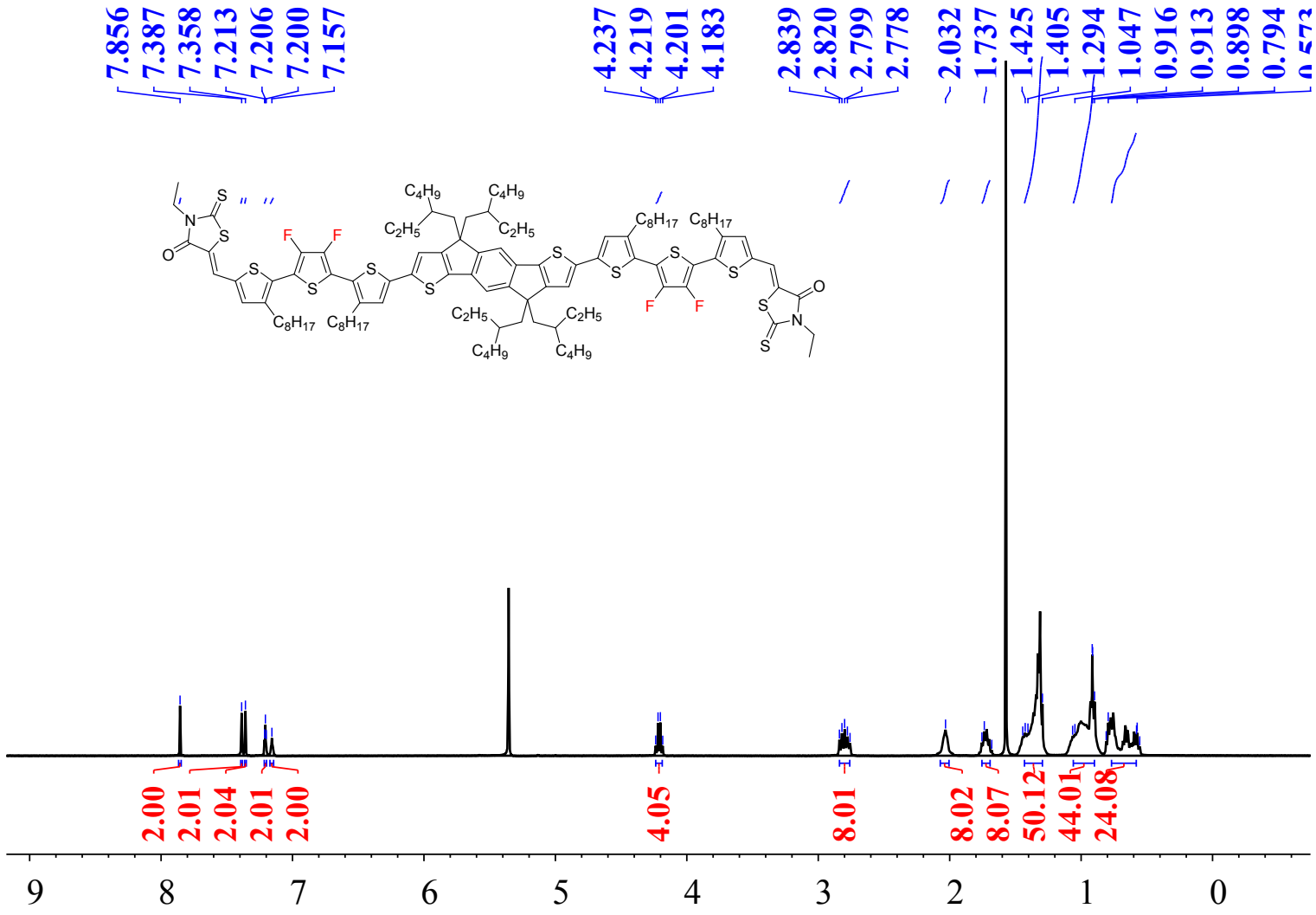

Figure S23. ^{1}H NMR spectrum of **I4FR-EH** in CD_2Cl_2.

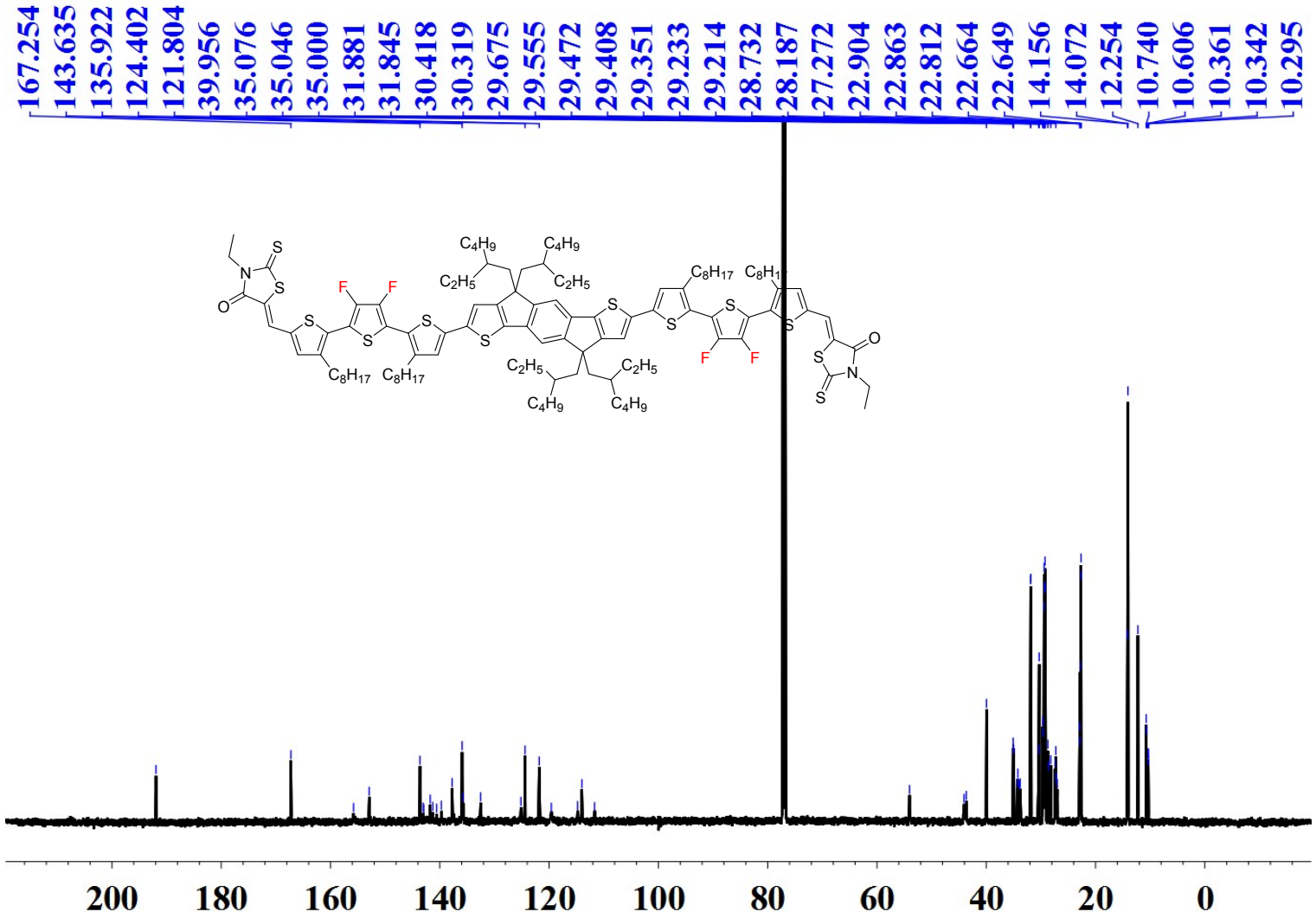

Figure S24. ^{13}C NMR spectrum of **I4FR-EH** in $CDCl_3$.

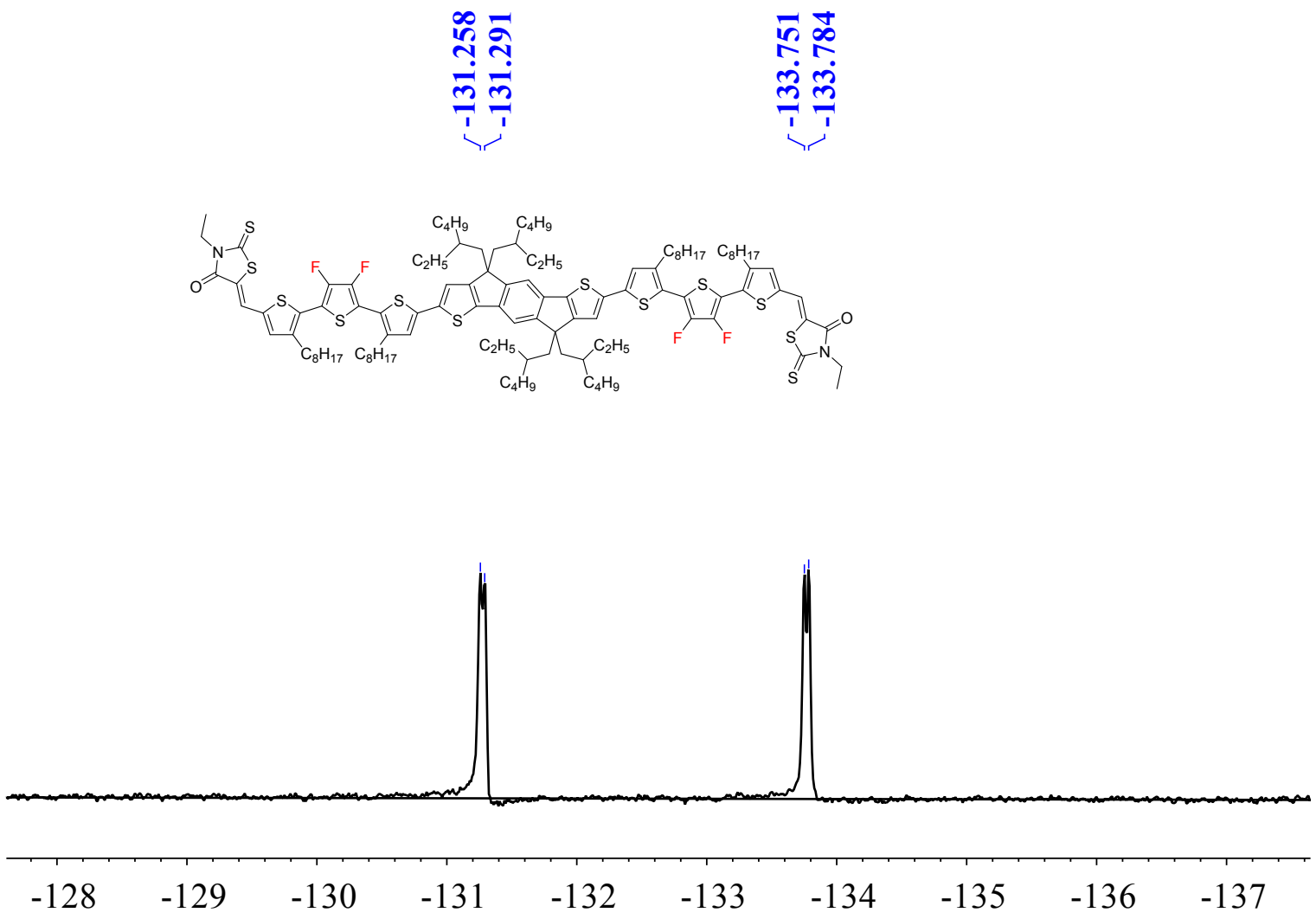

Figure S25. ^{19}F NMR spectrum of **I4FR-EH** in CD_2Cl_2.

8. Supporting Information References

[1] S. J. Liu, Z. P. Kan, S. Thomas, F. Cruciani, J. L. Brédas, P. M. Beaujuge, *Angew. Chem. Int. Edit.* **2016**, *55*, 12996-13000.

[2] H. Bronstein, D. S. Lee, R. Hamilton, P. Woebkenberg, S. King, W. M. Zhang, R. S. Ashraf, M. Heeney, T. D. Anthopoulos, J. de Mello, I. McCulloch, *Macromolecules* **2011**, *44*, 6649-6652.

[3] W. M. Zhang, J. Smith, S. E. Watkins, R. Gysel, M. McGehee, A. Salleo, J. Kirkpatrick, S. Ashraf, T. Anthopoulos, M. Heeney, I. McCulloch, *J. Am. Chem. Soc.* **2010**, *132*, 11437-11439.

[4] J. Pommerehne, H. Vestweber, W. Guss, R. F. Mahrt, H. Bassler, M. Porsch, J. Daub, *Adv. Mater.* **1995**, *7*, 551-554.